Arctic – Atlantic exchange of the dissolved micronutrients Iron, Manganese, Cobalt, Nickel, Copper and Zinc with a focus on Fram Strait

Stephan Krisch, Mark Hopwood, Stéphane Roig, Loes J.A. Gerringa, Rob Middag, Michiel Rutgers van Der Loeff, Mariia Petrova, Pablo Lodeiro, Manuel Colombo, Jay Cullen, et al.

Global Biogeochemical Cycles®

RESEARCH ARTICLE
10.1029/2021GB007191

Special Section:
The Arctic: An AGU Joint Special Collection

Arctic – Atlantic Exchange of the Dissolved Micronutrients Iron, Manganese, Cobalt, Nickel, Copper and Zinc With a Focus on Fram Strait

Stephan Krisch[1,2], Mark J. Hopwood[1], Stéphane Roig[1], Loes J. A. Gerringa[3], Rob Middag[3], Michiel M. Rutgers van der Loeff[4], Mariia V. Petrova[5], Pablo Lodeiro[1,6], Manuel Colombo[7], Jay T. Cullen[8], Sarah L. Jackson[8,9], Lars-Eric Heimbürger-Boavida[5], and Eric P. Achterberg[1]

[1]GEOMAR Helmholtz Centre for Ocean Research Kiel, Kiel, Germany, [2]Now at Bundesanstalt für Gewässerkunde, Koblenz, Germany, [3]NIOZ Royal Netherlands Institute for Sea Research, Den Burg, The Netherlands, [4]Alfred-Wegener-Institute for Polar and Marine Research, Bremerhaven, Germany, [5]Aix Marseille Université, CNRS/INSU, Université, de Toulon, IRD, Mediterranean Institute of Oceanography (MIO) UM 110, Marseille, France, [6]Department of Chemistry, University of Lleida – AGROTECNIO-CERCA Center, Lleida, Spain, [7]Department of Earth, Ocean, and Atmospheric Sciences, University of British Columbia, Vancouver, BC, Canada, [8]School of Earth and Ocean Sciences, University of Victoria, Victoria, BC, Canada, [9]Research School of Earth Sciences, Australian National University, Canberra, ACT, Australia

Key Points:

- Fram Strait is the major gateway for Arctic-Atlantic exchange of the dissolved micronutrients Fe, Mn, Co, Ni, Cu and Zn
- The Arctic is a net source of dissolved Fe, Co, Ni and Cu to the Nordic Seas and toward the North Atlantic; Mn and Zn exchange are balanced
- Waters of the Central Arctic Ocean, including the Transpolar Drift, are the main drivers of gross Arctic micronutrient export

Supporting Information:

Supporting Information may be found in the online version of this article.

Correspondence to:

S. Krisch and E. P. Achterberg,
stephankrisch.sk@gmail.com;
eachterberg@geomar.de

Citation:

Krisch, S., Hopwood, M. J., Roig, S., Gerringa, L. J. A., Middag, R., Rutgers van der Loeff, M. M., et al. (2022). Arctic – Atlantic exchange of the dissolved micronutrients iron, manganese, cobalt, nickel, copper and zinc with a focus on Fram Strait. *Global Biogeochemical Cycles*, *36*, e2021GB007191. https://doi.org/10.1029/2021GB007191

Received 16 SEP 2021
Accepted 28 APR 2022

Author Contributions:

Conceptualization: Stephan Krisch, Mariia V. Petrova, Lars-Eric Heimbürger-Boavida, Eric P. Achterberg
Formal analysis: Stephan Krisch, Stéphane Roig, Rob Middag, Michiel M. Rutgers van der Loeff, Pablo Lodeiro,

Abstract The Arctic Ocean is considered a source of micronutrients to the Nordic Seas and the North Atlantic Ocean through the gateway of Fram Strait (FS). However, there is a paucity of trace element data from across the Arctic Ocean gateways, and so it remains unclear how Arctic and North Atlantic exchange shapes micronutrient availability in the two ocean basins. In 2015 and 2016, GEOTRACES cruises sampled the Barents Sea Opening (GN04, 2015) and FS (GN05, 2016) for dissolved iron (dFe), manganese (dMn), cobalt (dCo), nickel (dNi), copper (dCu) and zinc (dZn). Together with the most recent synopsis of Arctic-Atlantic volume fluxes, the observed trace element distributions suggest that FS is the most important gateway for Arctic-Atlantic dissolved micronutrient exchange as a consequence of Intermediate and Deep Water transport. Combining fluxes from FS and the Barents Sea Opening with estimates for Davis Strait (GN02, 2015) suggests an annual net southward flux of 2.7 ± 2.4 Gg·a^{-1} dFe, 0.3 ± 0.3 Gg·a^{-1} dCo, 15.0 ± 12.5 Gg·a^{-1} dNi and 14.2 ± 6.9 Gg·a^{-1} dCu from the Arctic toward the North Atlantic Ocean. Arctic-Atlantic exchange of dMn and dZn were more balanced, with a net southbound flux of 2.8 ± 4.7 Gg·a^{-1} dMn and a net northbound flux of 3.0 ± 7.3 Gg·a^{-1} dZn. Our results suggest that ongoing changes to shelf inputs and sea ice dynamics in the Arctic, especially in Siberian shelf regions, affect micronutrient availability in FS and the high latitude North Atlantic Ocean.

Plain Language Summary Recent studies have proposed that the Arctic Ocean is a source of micronutrients such as dissolved iron (dFe), manganese (dMn), cobalt (dCo), nickel (dNi), copper (dCu) and zinc (dZn) to the North Atlantic Ocean. However, data at the Arctic Ocean gateways including Fram Strait and the Barents Sea Opening have been missing to date and so the extent of Arctic micronutrient transport toward the Atlantic Ocean remains unquantified. Here, we show that Fram Strait is the most important gateway for Arctic-Atlantic micronutrient exchange which is a result of deep water transport at depths >500 m. Combined with a flux estimate for Davis Strait, this study suggests that the Arctic Ocean is a net source of dFe, dNi and dCu, and possibly also dCo, toward the North Atlantic Ocean. Arctic-Atlantic dMn and dZn exchange seems more balanced. Properties in the East Greenland Current showed substantial similarities to observations in the upstream Central Arctic Ocean, indicating that Fram Strait may export micronutrients from Siberian riverine discharge and shelf sediments >3,000 km away. Increasing Arctic river discharge, permafrost thaw and coastal erosion, all consequences of ongoing climate change, may therefore alter future Arctic Ocean micronutrient transport to the North Atlantic Ocean.

1. Introduction

Fram Strait is situated between Svalbard and NE Greenland, and functions as a major gateway for water exchange between the Arctic Ocean and the North Atlantic Ocean (Rudels, 2019; Tsubouchi et al., 2018). The North Atlantic Ocean plays a central role in the meridional overturning circulation (Fu et al., 2020; Thornalley et al., 2018).

Manuel Colombo, Jay T. Cullen, Sarah L. Jackson
Funding acquisition: Eric P. Achterberg
Investigation: Stephan Krisch
Methodology: Stephan Krisch, Mariia V. Petrova, Lars-Eric Heimbürger-Boavida, Eric P. Achterberg
Project Administration: Eric P. Achterberg
Supervision: Mark J. Hopwood, Eric P. Achterberg
Validation: Stephan Krisch
Visualization: Stephan Krisch
Writing – original draft: Stephan Krisch
Writing – review & editing: Stephan Krisch, Mark J. Hopwood, Loes J. A. Gerringa, Rob Middag, Michiel M. Rutgers van der Loeff, Mariia V. Petrova, Pablo Lodeiro, Manuel Colombo, Jay T. Cullen, Sarah L. Jackson, Lars-Eric Heimbürger-Boavida, Eric P. Achterberg

Intermediate and deep Atlantic waters that ultimately reach the Arctic Ocean possess young ventilation ages with lower concentrations of nutrients and many trace elements compared to, for example, deep North Pacific waters (Achterberg et al., 2021; Ezoe et al., 2004). The Arctic Ocean comprises only 3% of the global ocean by area (Menard & Smith, 1966), but receives a disproportionally large fraction of global riverine discharge (~11%, Aagaard & Carmack, 1989) with ~50% of the Arctic Ocean's surface area being shelf seas (Jakobsson, 2002). Large rivers such as the Lena, Ob and Yenisei transport high loads of organic material (Amon et al., 2012) and micronutrient trace elements including iron (Fe), manganese (Mn), cobalt (Co), nickel (Ni), copper (Cu) and zinc (Zn) to Arctic Ocean shelf regions (Dai & Martin, 1995; Garnier et al., 1996; Guieu et al., 1996). Even after substantial flocculation and losses of some dissolved micronutrients in estuaries (e.g., >90% for dissolved Fe (dFe) in the Lena River, Conrad et al., 2019), a substantial flux of dFe, dissolved Mn (dMn), dissolved Co (dCo), dissolved Ni (dNi), dissolved Cu (dCu) and dissolved Zn (dZn) enters the Arctic annually from rivers, shelf sediments and coastal erosion (Charette et al., 2020; Gerringa, Rijkenberg, et al., 2021). A plume with elevated concentrations of shelf-derived radium and micronutrients including dFe and dCo, which are effectively stabilized by organic complexation, is subsequently advected offshore across the central Arctic Ocean within the Transpolar Drift (Bundy et al., 2020; Slagter et al., 2017). This results in pronounced near-surface dFe and dCo concentration maxima in the Central Arctic Ocean (Charette et al., 2020; Kadko et al., 2019; Klunder, Bauch, et al., 2012) and an inverted depth distribution of these elements compared to the North Atlantic (Achterberg et al., 2018, 2021; Rijkenberg et al., 2014). The southward extent of these elevated surface concentrations is so far undetermined. However, whilst surface drift pathways across the central Arctic Ocean are subject to considerable interannual variability (Wilson et al., 2021), recent repeat sections of radium indicate that the cross-Arctic transfer of shelf derived elements increased from 2007 to 2015 (Kipp et al., 2018), with potential consequences for micronutrient export through Fram Strait (Mauritzen et al., 2013; Rudels, 2019).

Volume exchange between the Arctic and the high latitude North Atlantic Oceans (>65°N) is controlled by three gateways: (a) Fram Strait (net southward flux of 1.1 ± 1.2 Sv), separating the Nordic Seas to the south from the Arctic Ocean, (b) Barents Sea Opening, located between Svalbard and coastal Norway (net northward flux of 2.3 ± 1.2 Sv), and (c) Davis Strait, separating the Labrador Sea to the south from Baffin Bay and the Canadian Arctic Archipelago (net southward flux of 2.1 ± 0.7 Sv) (Tsubouchi et al., 2018). Fram Strait is the only deep water connection with depths exceeding 500 m (Jakobsson et al., 2012) and thus facilitates intermediate and deep water exchange between the two ocean basins (Mauritzen et al., 2013; von Appen et al., 2015). Approximately two-thirds of northward flowing Atlantic Water (2.4–5.4 Sv) enters the Arctic Ocean through Fram Strait as part of the West Spitsbergen Current (WSC, 6.6 ± 0.4 Sv) which is formed by contributions from the Norwegian Atlantic Front Current and the coastal Norwegian Atlantic Slope Current (Figure 1; Beszczynska-Möller et al., 2012; Rudels, 2019). The remaining fraction (1.5–2 Sv) enters the Arctic Ocean via the Barents Sea Opening ("Barents Sea Branch") which is mostly derived from the Norwegian Atlantic Slope Current (Rudels, 2019). In Fram Strait, low-salinity Polar Surface Water, cooled and freshened Arctic Atlantic Water, together with locally recirculating Atlantic Water, forms the East Greenland Current (EGC, 8.7 ± 2.5 Sv at 78°50'N, de Steur et al. (2014)), which is the main southward Arctic Ocean outflow into the North Atlantic (Laukert et al., 2017; Richter et al., 2018; Rudels et al., 2005). With seasonal variation, ~30%–50% of the total annual net Arctic Ocean outflow occurs through Fram Strait (Rudels, 2019).

Over the last three decades, Atlantic Water volume transport to the Arctic Ocean across Fram Strait has been stable (Tsubouchi et al., 2021) suggesting minor decadal-scale changes related to anthropogenic climate change. In contrast, the Arctic is currently undergoing rapid change as a consequence of atmospheric and oceanic warming (IPCC, 2019). Increasing riverine discharges (Rawlins et al., 2010) with elevated concentrations of trace elements (Dai & Martin, 1995; Guieu et al., 1996), and increasing supply of organic matter (Feng et al., 2013) containing trace element-binding ligands (Slagter et al., 2017), may result in enhanced micronutrient concentrations in Polar Surface Water and increase lateral dFe, dMn, dCo, dNi, dCu and dZn transport toward Fram Strait (Charette et al., 2020; Kipp et al., 2018). Presently, Fram Strait also accounts for >90% of all Arctic Ocean sea ice export (Kwok, 2009), with the areal extent of exported ice increasing since 1979 (+6% per decade, Smedsrud et al., 2017) - although export of sea ice formed in shallow areas of the Arctic Ocean is declining (−17% per decade since 1998, Krumpen et al., 2019). Overall decreasing sea ice cover may facilitate enhanced primary production and the associated micronutrient drawdown within the Arctic (Lewis et al., 2020). Furthermore, sea ice functions as a vehicle for lateral shelf-sediment transport (Dethleff & Kuhlmann, 2010) and may release substantial quantities of dissolved and particulate micronutrients to the surface ocean during the melt season

Table 1
Measured Concentrations (in nmol L^{-1}, nM) and Standard Deviations (±1σ) of Fe, Mn, Co, Ni, Cu and Zn for Reference Materials SAFe D1 (GN04), SAFe S and GSC (GN05); n = Number of Measurements

Reference material	Analyte	Consensus[a]	Measured	n
GN04 SAFe D1 (#599)	Fe	0.69 ± 0.04	0.82 ± 0.04	6
	Mn[b]	0.43 ± 0.02	0.41 ± 0.002	6
	Co	0.0466 ± 0.0048	0.0432 ± 0.0019	6
	Ni	8.80 ± 0.27	8.76 ± 0.09	6
	Cu	2.31 ± 0.11	2.04 ± 0.02	6
	Zn	7.59 ± 0.36	7.53 ± 0.05	6
GN05 SAFe S (#273)	Fe	0.095 ± 0.008	0.101 ± 0.016	10
	Mn	0.81 ± 0.06	0.87 ± 0.18	10
	Co	0.0049 ± 0.0012	0.0063 ± 0.0018	10
	Ni	2.34 ± 0.09	2.26 ± 0.20	9
	Cu	0.53 ± 0.05	0.52 ± 0.03	11
GSC (#21, #159)	Zn[b]	1.41 ± 0.10	1.37 ± 0.14	7

[a]Conversion from nmol kg^{-1} by density of 1.026 kg L^{-1}. [b]Value obtained from Wuttig et al. (2019).

(Tovar-Sánchez et al., 2010; Wang et al., 2014). The end result of the synergistic effects between sea ice loss, and micronutrient supply and demand is therefore challenging to predict. Future projections suggest the loss of sea ice cover may also result in increased advection of Atlantic Water across the Nordic Seas into the Arctic Ocean (Wang et al., 2020) contributing to Arctic "Atlantification" (Ricker et al., 2021). How these changes will affect dFe, dMn, dCo, dNi, dCu and dZn exchange remains unknown due to a lack of trace element data across Fram Strait.

The present study forms part of the international GEOTRACES program, and focuses on the distribution and advection of dFe, dMn, dCo, dNi, dCu and dZn in water masses of the Fram Strait (cruise GN05) and Barents Sea Opening (cruise GN04). Among the micronutrients, Fe is of particular interest as its availability limits summertime primary production in large parts of the North Atlantic Ocean including the Iceland and Irminger Basin (Browning et al., 2019; Nielsdóttir et al., 2009; Ryan-Keogh et al., 2013). Furthermore, parts of the Arctic Ocean were suggested to be deficient in dFe relative to average phytoplankton requirements (Nansen Basin, Rijkenberg et al., 2018) or display some evidence of Fe co-limitation (Beaufort Sea, Taylor et al., 2013). Whilst nitrate and dFe availability are thought to be the main (co-)limiting nutrients for primary production across the Arctic and North Atlantic (Randelhoff et al., 2020; Taylor et al., 2013), in other parts of the global surface ocean, phytoplankton community growth is (co-)limited by dMn (Southern Ocean, Browning et al., 2021; Wu et al., 2019) and dCo (North- and South-Atlantic, Browning et al., 2017; Panzeca et al., 2008). The availability of dNi (Dupont et al., 2010), dCu (Brand et al., 1986; Sanders et al., 1981) and dZn (Crawford et al., 2003) may also influence phytoplankton species composition and primary production (Brand et al., 1986; Sanders et al., 1981), raising questions about how broad-scale changes as a result of Arctic amplification and "Atlantification" will affect the supply and distribution of micronutrients.

Combined with the most recent year-round synopsis of Arctic-North Atlantic volume transport fluxes, here we calculate the associated dFe, dMn, dCo, dNi, dCu and dZn fluxes for the Fram Strait and Barents Sea Opening gateways. For comparison, we also estimated net fluxes for Davis Strait using available GEOTRACES data (GN02, 2015) from stations within the Baffin Current. The aim of this study is to establish a baseline against future changes in dissolved micronutrient fluxes between the Arctic and Atlantic Oceans and to determine the water mass components contributing most to the net and gross fluxes. To our best knowledge, this is the first attempt to quantify micronutrient exchanges between the Arctic and North Atlantic Oceans.

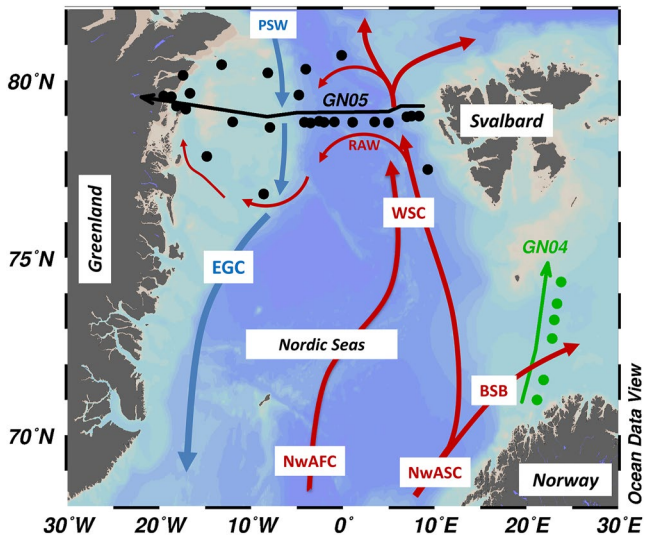

Figure 1. Schematic of current flow paths, and location of stations sampled during GEOTRACES expeditions GN05 (2016) in Fram Strait (FS) (black circles), and GN04 (2015) in the Barents Sea Opening (green circles). Thin arrows highlight the sections which are shown in Figure 2 (FS, GN05, in black) and in Figure S4 in Supporting Information S1 (Barents Sea Opening, GN04, in green). Warm, saline (cold, fresher) Atlantic-derived (Arctic-derived) currents are depicted in bold-red (bold-blue): Norwegian Atlantic Front Current Current (NwAFC), Norwegian Atlantic Slope Current (NwASC), Barents Sea Branch (BSB), West Spitsbergen Current (WSC), Recirculating Atlantic Water (RAW), Polar Surface Water (PSW), East Greenland Current (EGC). Station numbers, and stations in the Central Arctic Ocean are shown in Figure S1 in Supporting Information S1.

2. Methods

2.1. Sampling

Samples were collected during two GEOTRACES expeditions in 2015 (section GN04, 17 August–15 October), and 2016 (GN05, 21 July–6 September) on-board the research icebreaker Polarstern (Figure 1, Figure S1 in Supporting Information S1). On cruise GN05, a transect was conducted from the West Svalbard shelf toward coastal NE Greenland covering Fram Strait at 78°50'N and the NE Greenland Shelf (e.g., Ardiningsih et al., 2020; Krisch et al., 2020). Four stations were located within the WSC (>5°E), nine stations within the EGC (6.5°W–2°E), with one station in between ("Middle", 2–5°E), and 12 stations on the NE Greenland Shelf (>6.5°W) (Kanzow, 2017). In the scope of this study, GN04 investigated the Barents Sea Opening through a transect of six stations near the continental shelf break between coastal Norway and Hopen Island (Svalbard) (Schauer, 2016). Three additional stations were occupied during cruise GN04 in the central Arctic Ocean Transpolar Drift around 90°N (stations 81, 91, and 96 as per Gerringa, Rijkenberg, et al., 2021).

On GN05, micronutrient sampling was conducted using a powder-coated aluminum GEOTRACES frame (Seabird, equipped with a SBE 911 CTD) with 24 × 12 L GoFlo bottles (Cutter et al., 2017). Micronutrient sampling on GN04 used the titanium NIOZ frame (equipped with a Seabird SBE 911) and 24 × 24 L polyvinylidene fluoride samplers (Rijkenberg et al., 2015). Vertical, full depth profiles of salinity, temperature, pressure and light attenuation (turbidity) were conducted at high-resolution on both expeditions. Following GEOTRACES sampling protocols (Cutter et al., 2017), both expeditions sampled the water column to full depth and utilized an over-pressured class 100 ultraclean laboratory container for subsampling immediately after deployment. Samples were filtered into pre-cleaned LDPE (low density polyethylene) 125 mL bottles using Acropak™ 500/1000 capsules with hydrophilic PES-membrane (0.8/0.2 µm pore size; Pall Corp.) on GN05 and Sartobran® 300 capsules with hydrophilic cellulose acetate membrane (0.45/0.2 µm pore size; Sartorius) on GN04. Following filtration, samples were acidified to pH 1.9 (GN05) or pH 1.8 (GN04) with ultrapure HCl (GN05: ROMIL, GN04: Seastar Chemicals Inc.) and shipped to GEOMAR (GN05) and NIOZ (GN04) for subsequent dissolved micronutrient analysis.

Both expeditions also retained samples for macronutrient analyses of nitrate (NO_3), phosphate (PO_4) and silicic acid ($Si(OH)_4$, in the following referred to as dSi) from each water sample bottle. During GN05, macronutrient samples above 200 m depth remained unfiltered and were analyzed on-board using a QuAAtro autoanalyser as per Grasshoff et al. (1999), modified according to the methods provided by the manufacturer (Seal, Alliance). Samples at all other depths were filtered (Acropak™ 500/1000 capsules; Pall Corp.), frozen and analyzed at AWI in an identical procedure. Macronutrient measurements were validated against NMIJ CRM 7602a reference material obtained from the National Metrology Institute of Japan (see data publication). On GN04, macronutrient samples were retained without filtration and analyzed immediately after sampling using a Technicon TRAACS 800 auto-analyzer as described by Rijkenberg et al. (2018). GN04 macronutrient measurements were validated against Kanso Technos, lot BU and lot BT, reference material (see data publication).

Samples for radium isotope analyses (^{226}Ra, ^{228}Ra) were collected from GN04 and GN05 following standardized GEOTRACES protocols (Cutter et al., 2017) and measured via gamma spectrometry as previously described by Rutgers van der Loeff et al. (2018) (GN04) and Krisch, Hopwood, et al. (2021) (GN05). On GN05 only, samples for the analyses of stable oxygen isotopes ($\delta^{18}O$) were obtained (Cutter et al., 2017) and analyzed via mass spectrometry following the procedure as described in Meyer et al. (2000).

2.2. Micronutrient Analyses

Dissolved micronutrient concentrations in samples collected during cruise GN05 were analyzed via high-resolution inductively coupled plasma-mass spectrometry (HR-ICP-MS) following solid-phase extraction, exactly as per Rapp et al. (2017). Briefly, 10 mL sample aliquots were UV-digested to liberate micronutrients from strong organic complexation, and pre-concentrated using an automated SeaFAST system (SC4 DX SeaFAST pico; ESI). All reagents for SeaFAST were prepared in deionized water (>18.2 MΩ cm; Milli-Q, Millipore). Single-distilled sub-boiled HNO_3 (SpA grade, Romil) was used for sample elution. Ammonium acetate buffer was prepared from glacial acetic acid and ammonium hydroxide (Optima grade, Fisher Scientific). The 10-fold preconcentrated samples were analyzed by HR-ICP-MS (Thermo Fisher Element XR). Calibration was via isotope dilution for Fe, Ni, Cu and Zn, and standard addition for Mn and Co (Inorganic Ventures standard solutions).

Samples from GN04 were analyzed via solid-phase extraction and HR-ICP-MS (Thermo Finnigan Element 2) as described in Gerringa, Rijkenberg, et al. (2021). Briefly, 30 mL of UV-digested sample were pre-concentrated using an automated SeaFAST system (SC4 DX SeaFAST pico; ESI) through addition of ammonium acetate buffer that was prepared from ammonium hydroxide and sub-boiled glacial acetic acid (Suprapur grade, Merck). All reagents were prepared in deionized water (>18.2 MΩ cm; Milli-Q, Millipore). The 40-fold pre-concentrated samples were eluted using double-distilled sub-boiled HNO_3 (Suprapur grade, Merck) and analyzed by HR-ICP-MS. Calibration for Fe, Mn, Co, Ni, Cu and Zn was via standard addition from a mixed standard, made from single spike standards (TraceCERT, Sigma-Aldrich).

Validation of method accuracy for micronutrient analyses was through GEOTRACES SAFe D1 (GN04), SAFe S and GSC (GN05) reference materials (Bruland Research Lab, 2009) (Table 1). In-house reference seawater CAB (GN05) and NADW (GN04) were used to monitor long-term precision (Table S1 in Supporting Information S1). Procedural blank contribution was determined by HR-ICP-MS analyses of 1 M HNO_3 (elution acid) obtained from SeaFAST where the sample introduction step was omitted from the pre-concentration method and includes contribution from the SeaFAST buffer (GN05), or from acidified de-ionized water (pH 1.8) treated as a "regular" sample to SeaFAST pre-concentration (GN04) (Table S2 in Supporting Information S1). Limits of detection were defined as three times the standard deviation of the blank.

2.3. Flux Calculations

Calculations of dFe, dCo, dMn, dNi, dCu and dZn fluxes through the Fram Strait, Barents Sea Opening, and Davis Strait are based on monthly mean volume transport estimated from mooring observations for the period September 2005–August 2006 (Tsubouchi et al., 2018) and concentrations observed along the cruise sections GN04 and GN05. Water masses of Fram Strait, that is, WSC (>5°E), Middle section (2–5°E), EGC (2°E–6.5°W), and the NE Greenland Shelf (>6.5°W) are differentiated into layers ("components") of Surface Water ($\sigma_0 < 27.1$ kg/m^3), Upper Atlantic Water ($27.10\sigma_0$–$27.50\sigma_0$ kg/m^3), Atlantic Water ($27.50\sigma_0$–$30.28\sigma_{0.5}$ kg/m^3), Intermediate Water ($30.28\sigma_{0.5}$–$32.75\sigma_{1.0}$ kg/m^3), and Deep Water ($\sigma_{1.0} > 32.75$ kg/m^3) by definition of isopycnal surfaces and potential density relative to 0 dbar (σ_0), 500 dbar ($\sigma_{0.5}$) and 1000 dbar ($\sigma_{1.0}$) using GN04 and GN05 CTD data following Tsubouchi et al. (2018) (Figure 2). The water column of the Barents Sea Opening is analogously distinguished into layers but treated as one water mass ("Barents Sea Branch") in accordance with Petrova et al. (2020).

Micronutrient fluxes were calculated using volume transport rates, and concentrations of dFe, dMn, dCo, dNi, dCu and dZn for each individual water mass within each component. Monthly mean micronutrient fluxes were calculated from monthly mean volume transport rates multiplied by the average dissolved micronutrient concentrations from the sampling campaigns in October 2015 (Barents Sea Opening, GN04) and July–September 2016 (Fram Strait, GN05). The uncertainty in August micronutrient transport across Fram Strait was calculated from error propagation including the uncertainty in dissolved micronutrient concentrations, and an estimate of uncertainty in volume transport derived from assuming proportionality between volume transport rates in August 2006 and mean variability in volume transport as observed between September 2005 and August 2006 (Tsubouchi et al., 2018). To establish annual dFe, dMn, dCo, dNi, dCu and dZn fluxes, we average over monthly mean net micronutrient fluxes (September–August, in Gg·a^{-1}) and report uncertainty as one standard deviation (1σ) of monthly variations following Petrova et al. (2020). This is because the Arctic Ocean is a closed system where volume fluxes are not independent variables. Classical error propagation would lead to an over-estimation in the calculated error for net annual Arctic-Atlantic micronutrient exchange. We explore the potential implications of

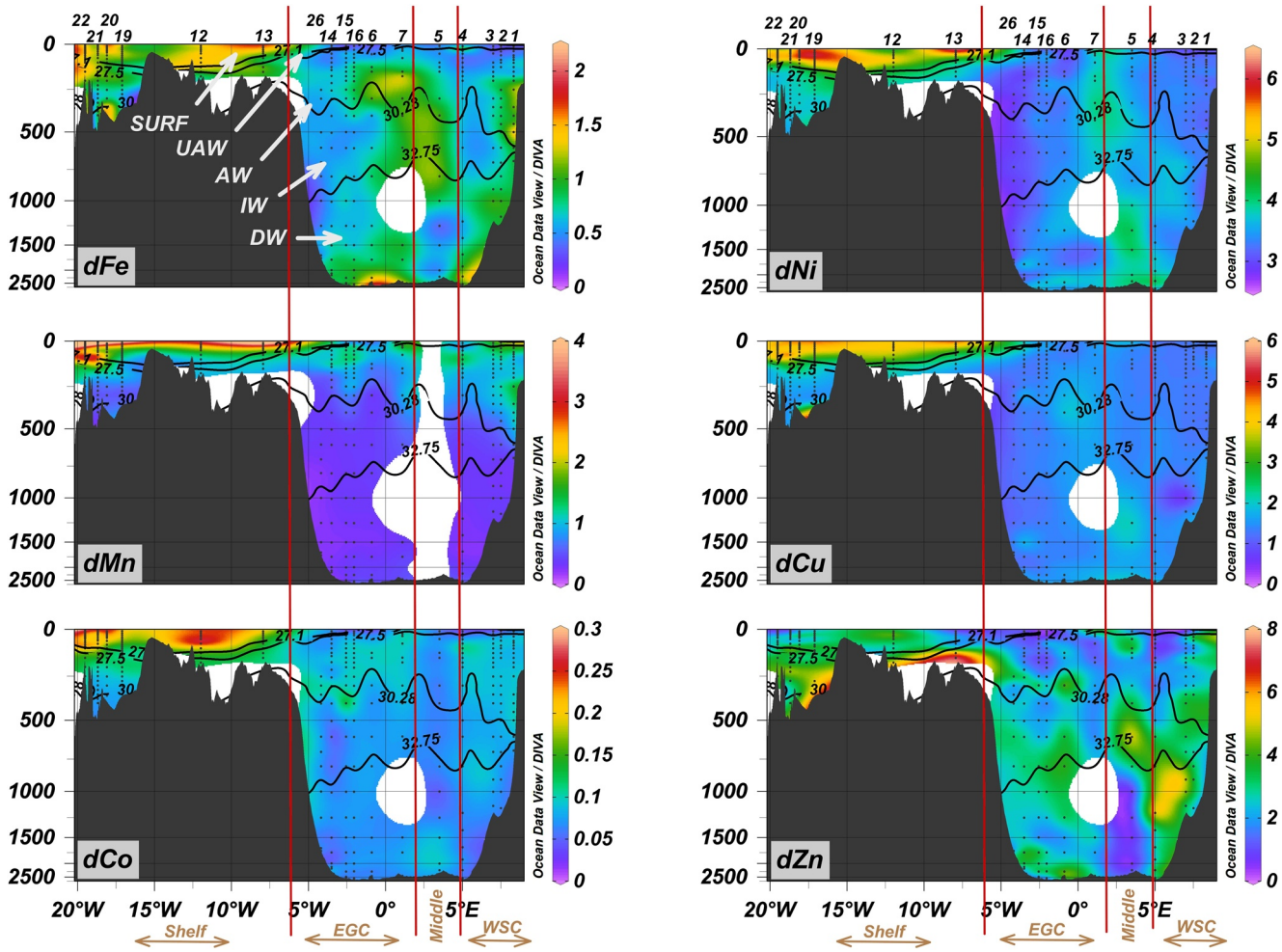

Figure 2. Dissolved distribution of Fe (top left), Mn (central left), Co (bottom left), Ni (top right), Cu (central right) and Zn (bottom right) in FS at 79°N (GN05). All concentrations indicated by color are in nmol L^{-1}. Section plotted as indicated in Figure 1 ("Section GN05"). Sample depths used for interpolation are shown as black dots. Station numbers indicated in top panel. Isopycnal surfaces (blank contours), derived from CTD measurements, distinguish between water masses: Surface Water (SURF, $\sigma_0 < 27.1$ kg/m^3), Upper Atlantic Water (UAW, 27.10σ_0–27.50σ_0 kg/m^3), Atlantic Water (AW, 27.50σ_0–30.28$\sigma_{0.5}$ kg/m^3), Intermediate Water (IW, 30.28$\sigma_{0.5}$–32.75$\sigma_{1.0}$ kg/m^3) and Deep Water (DW) (DW, $\sigma_{1.0} > 32.75$ kg/m^3). Vertical red lines delineate the West Spitsbergen Current (WSC, >5°E), the Middle (2–5°E), the East Greenland Current (EGC, 6.5°W–2°E) and the NE Greenland Shelf (>6.5°W) following the definitions of Tsubouchi et al. (2018). The Barents Sea Opening section is found in the Supplementary Information (Figure S4 in Supporting Information S1).

seasonal variations for annual fluxes based on the limited multi-seasonal micronutrient data available for the high latitude North Atlantic (Achterberg et al., 2018, 2021).

3. Results and Discussion

3.1. Micronutrient Distributions

In Fram Strait, Surface Water was absent in the WSC and increased in thickness from western Fram Strait toward Greenland (Figure 2). Upper Atlantic Water formed the surface layer in the WSC and also increased in thickness toward the Greenlandic coast. Atlantic Water was present across the section and increased in thickness toward eastern Fram Strait and the Atlantic-sourced WSC. Intermediate Waters were observed across Fram Strait and deeper parts (i.e., troughs) of the NE Greenland Shelf. The layer of Intermediate Water was thickest in the EGC. Deep Water layer thickness varied little in the deeper parts of Fram Strait (>630 m), and Deep Water was absent elsewhere.

The distribution of dFe in Fram Strait (Figure 2, Table S3 in Supporting Information S1) showed a pronounced gradient of decreasing concentrations with depth in the EGC (range: 0.19–3.04 nM) and on the NE Greenland Shelf (0.49–3.35 nM), in agreement with observations in the Central Arctic Ocean (Klunder, Bauch, et al., 2012; Rijkenberg et al., 2018). Both water masses contrast starkly with the increase in dFe concentrations with depth observed elsewhere across the Atlantic, Pacific and Southern Oceans away from the confounding influence of regional shelf or hydrothermal sources (Rijkenberg et al., 2014; Schlitzer et al., 2018). Conversely, in the WSC (0.22–1.94 nM) dFe concentrations increased with depth, which is more typical for Atlantic waters due to biological drawdown in surface waters and remineralization at depth (Rijkenberg et al., 2014; Tonnard et al., 2020). An east-to-west gradient in surface dFe was consequently evident. Dissolved Fe maxima were observed in the Surface Waters of the EGC (1.02 ± 0.62 nM, mean concentration ± standard deviation (1σ)) near the Greenland continental slope (1.32 ± 0.35 nM at stations 9–10, 12–13 and 25) and on the NE Greenland Shelf proximal to the Nioghalvfjerdsbrae and Zachariæ Isstrøm glacier outflows (1.65 ± 0.58 nM at stations 20, 22 and 24). Further east, Upper Atlantic Water exhibited a pronounced dFe minimum in the surface WSC (0.22 ± 0.01 nM at 10 m, station 4), potentially as a consequence of elevated primary production in eastern Fram Strait (Krisch et al., 2020). Differences in phytoplankton drawdown, as suggested from the gradient in species distribution (Krisch et al., 2020), may have additionally contributed to the east-to-west gradient in surface dFe concentrations across Fram Strait. Dissolved Fe within Atlantic Water and Intermediate Water was more uniformly distributed and showed comparatively little variation between the WSC (0.67 ± 0.32 nM, 0.64 ± 0.06 nM, respectively) and the NE Greenland Shelf (0.89 ± 0.26 nM, 0.85 ± 0.56 nM, respectively). Dissolved Fe maxima in Atlantic Water and Intermediate Water above the Svalbard (1.64 nM at 500 m, station 1) and Greenland shelf break (3.04 nM at 250 m, station 9; 2.64 nM at 225 m, station 25), and near the glacier termini of Nioghalvfjerdsbrae (∼1.5 nM at 100–150 m, station 22) and Zachariæ Isstrøm (2.40 nM at 355 m, station 20) indicate localized sedimentary inputs across the region, as have been observed in other Arctic shelf environments (Kondo et al., 2016; Laufer-Meiser et al., 2021; Vieira et al., 2019). Deep Water showed increasing dFe concentrations with depth across Fram Strait (range: 0.34–2.25 nM), potentially as a consequence of organic matter remineralization (Granskog et al., 2012) and sediment resuspension caused by mixing of waters (von Appen et al., 2015).

The vertical and horizontal distribution of dMn, dCo, dNi and dCu (Figure 2) showed partially similar trends to dFe in Fram Strait. As was the case for dFe, an east-to-west gradient was apparent with increasing concentrations toward the Greenlandic coast (Table S3 in Supporting Information S1). Maximum concentrations were observed in Surface Water on the NE Greenland Shelf (3.15 ± 2.23 nM dMn, 204 ± 49 pM dCo, 5.27 ± 0.56 nM dNi, 4.00 ± 0.61 nM dCu), with dMn and dCo most elevated in Surface Water near the glacier termini of Nioghalvfjerdsbrae and Zachariæ Isstrøm (4.15 ± 2.67 nM dMn and 237 ± 45 pM dCo at stations 20, 22 and 24) contrasting with a rather homogenous horizontal distribution of dNi and dCu on the shelf. Dissolved Mn evidenced maxima in surface layers that were 3-6-fold elevated compared to mean bottom layer concentrations, and likely reflected near-surface inputs (Marsay et al., 2018; Middag et al., 2011; Wehrmann et al., 2014) and photochemical stabilization of dMn (Sunda & Huntsman, 1988) in surface Fram Strait. Conversely, dCo, dNi and dCu showed surface layer maxima and decreasing concentrations with depth only in the EGC and waters on the NE Greenland Shelf. There, Surface Water were 1.7–2.7-fold (dCo), ∼1.4-fold (dNi) and 2–2.5-fold (dCu) enriched relative to mean bottom layer concentrations, potentially related to glacial meltwater addition (Krause et al., 2021) and sea ice input (Tovar-Sánchez et al., 2010) and likely aided through organic stabilization of dCo (Bundy et al., 2020), dNi (Van Den Berg & Nimmo, 1987) and dCu (Coale & Bruland, 1988) in near-surface waters. In the WSC and parts of western Fram Strait, dCo showed surface layer minima (60 ± 10 pM in the WSC; 47 ± 12 pM at stations 6, 15 and 16) and subsurface layer maxima (86 ± 13 pM in the WSC, 93 ± 9 pM at stations 6, 15 and 16) which, corroborated by observations of increasing dNi and dCu concentrations with depth in the WSC, suggests the influence of drawdown by primary production and regeneration at depth (Krisch et al., 2020).

Dissolved Zn mirrored the general distribution of dFe, dMn, dCo, dNi and dCu across Fram Strait (Figure 2). Minima were observed in the surface layer and concentrations increased with depth, and toward Svalbard. An exemption to this trend was observed at station 5 covering the Middle section where dZn concentrations in Deep Water were depleted (0.99 ± 0.98 nM) compared to Atlantic Water (2.96 ± 0.79 nM), potentially capturing a separate water mass as suggested from the strong alternating current regimes observed between September 2005 and August 2006 in the central parts of Fram Strait (Tsubouchi et al., 2018). Depleted dZn in EGC Surface Water (1.21 ± 0.56 nM) and Upper Atlantic Water (1.02 ± 0.51 nM) contrasted with the WSC where surface (Atlantic Water) dZn was ∼2-fold elevated (Table S3 in Supporting Information S1). Mean dZn concentrations in the EGC

(2.16 ± 1.10 nM for all stations between 2°E–6.5°W) were similar to observations in the WSC (2.52 ± 1.27 nM for all stations >5°E). This was a clear contrast with the water column on the NE Greenland Shelf where dZn was most elevated (3.03 ± 1.42 nM for all stations >6.5°W) indicative of a shelf sediment source (Vieira et al., 2019). On the shelf, dZn maxima were observed in the bottom water of the North-East Water Polynya (5.22 ± 0.35 nM in Atlantic Water of station 11), a productive region near coastal Greenland, and close to the seafloor near the Greenland continental margin (5.30 ± 1.64 nM in waters >125 m depth at stations 12 and 13).

Increasing concentrations of dZn in waters on the NE Greenland Shelf correlated with increasing concentrations of dSi (0.517 ± 0.069 nM/μM, R^2 0.29 for all stations >6.5°W). This was particularly the case near coastal Greenland (0.835 ± 0.124 nM/μM, R^2 0.50 for stations 11, 19, 21 and 23) (Figures S2 and S3 in Supporting Information S1) were dZn/dSi was ~7-10-fold elevated relative to observations on the Bering and Chukchi Shelf Sea (0.076 ± 0.012 nM/μM, Jensen et al., 2019). This suggests a strong influence of sedimentary Zn sources and a decoupling of dZn from dSi inputs, perhaps as a consequence of preferential dissolution of Zn from biogenic particles in the water column (Jensen et al., 2019; Twining et al., 2014) on the NE Greenland Shelf. Regression slopes of dZn/dSi in the EGC (0.155 ± 0.032 nM/μM, R^2 0.13) were significantly lower and at the upper end of observations from the Central Arctic Ocean (range: −0.17 to 0.17 nM/μM, Gerringa, Rijkenberg, et al., 2021) including Arctic Ocean Polar Surface Water (0.129 nM/μM, R^2 0.72, Gerringa, Rijkenberg, et al., 2021) and Arctic Atlantic Water (0.133 nM/μM, R^2 0.32, Gerringa, Rijkenberg, et al., 2021), suggesting comparatively little influence of NE Greenland shelf sources on the general distribution of dZn beyond the shelf break. Dissolved Zn/dSi evidenced a slightly better correlation and a steeper slope in the WSC (0.273 ± 0.063 nM/μM, R^2 0.25 at stations 2–4) compared to observations in the EGC which may be linked to elevated primary production in eastern Fram Strait (Krisch et al., 2020).

In the shallow Barents Sea Opening, Atlantic Water was the dominant water mass and deepened closer to Svalbard (station 149), where it occupied the full water column (Figure S4 in Supporting Information S1). Surface Water was only observed near mainland Norway (station 173) making saline Upper Atlantic Water the main surface layer in the Barents Sea Opening. Intermediate and Deep Atlantic Waters were not present. The distribution of dFe, dMn, dCo, dNi, dCu and dZn in the Barents Sea Opening was similar to observations in the WSC of Fram Strait at similar depth. All dissolved micronutrients showed increasing concentrations from Svalbard toward mainland Norway where local maxima were observed. Concentrations of dFe, dCo, dNi and dZn generally increased with depth, in contrast to dMn and dCu which evidenced maxima in surface waters near mainland Norway. For a more detailed description, we refer the reader to Gerringa, Rijkenberg, et al. (2021) where the biogeochemical cycling of dFe, dMn, dCo, dNi, dCu and dZn in the Barents Sea Opening is discussed in greater detail.

Principal Component Analysis was conducted to investigate regional relationships between micronutrients (dFe, dMn, dCo, dNi, dCu and dZn), macronutrients (nitrate, phosphate and dSi) and salinity (Figure 3). For details on the distribution of macronutrients in Fram Strait, we refer the reader to the publication of Krisch et al. (2020). In Fram Strait, the two principal components PC1 and PC2 reflect 67.9% of variance in parameters in the WSC (41.8% for PC1 and 26.0% for PC2), 71.8% of variance in the EGC (48.2% for PC1 and 23.6% for PC2), and 76.2% of variance in waters on the NE Greenland Shelf (67.5% for PC1 and 8.7% for PC2). Controlling factors on dissolved micronutrient distributions evidenced an east-to-west gradient in Fram Strait. In the WSC, dissolved Fe, dNi, dCu and dZn grouped with depth and showed a less significant relationship with salinity, suggesting their distribution was influenced by biological uptake and scavenging in surface waters, and remineralization and sedimentary release processes at depth in agreement with findings from Krisch et al. (2020). Dissolved Co and dMn in the WSC were more positively correlated with salinity, and in the case of dMn grouped in opposition to depth, suggesting saline waters, and photo-dissolution processes in the surface ocean as dominant drivers (Moffett & Ho, 1996; Sunda & Huntsman, 1994). In the EGC and on the NE Greenland Shelf, dissolved Mn, dCo, dNi and dCu grouped in opposition to salinity suggesting strong influence by a common, low salinity source. As was the case in the WSC, dZn in the EGC and on the NE Greenland Shelf showed a close relationship with macronutrients, particularly with dSi. This is consistent with phytoplankton uptake of dZn followed by remineralization of dZn alongside phosphate and dSi (Middag et al., 2019; Weber et al., 2018) with little influence from low salinity sources. Dissolved Fe in the EGC and on the NE Greenland Shelf evidenced no clear correlation with either salinity or depth, and grouped in between dZn and macronutrients on the one hand, and dMn, dCo, dNi and dCu on the other hand. This suggests multiple factors such as biological activity (Krisch et al., 2020), low salinity sources

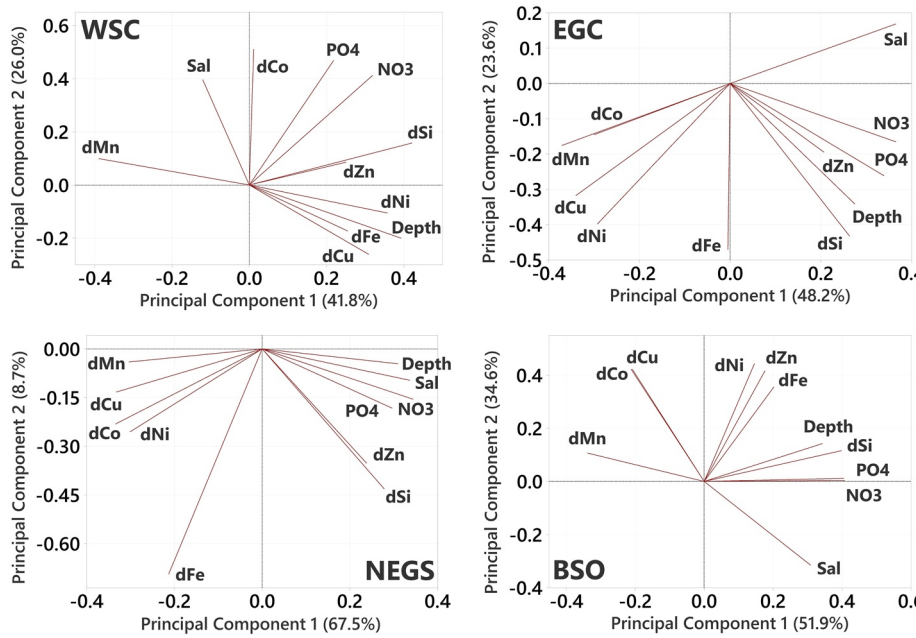

Figure 3. Principal Component Analysis (PCA) loading plots illustrating trends in the distribution of dissolved micronutrients (dFe, dMn, dCo, dNi, dCu and dZn) and macronutrients (nitrate, phosphate, dSi) relative to salinity (Sal) and depth in the water column of Fram Strait (GN05) and the Barents Sea Opening (GN04). Top left: West Spitsbergen Current (WSC); top right: East Greenland Current (EGC); bottom left: NE Greenland Shelf (NEGS); bottom right: Barents Sea Opening (BSO).

and sedimentary release into saline waters (Krisch, Hopwood, et al., 2021) are influencing the distribution of dFe in the western parts of Fram Strait.

In the Barents Sea Opening, a similar analysis of macronutrients, micronutrients, salinity and depth, but without Intermediate and Deep Water, yielded principal components with 51.9% (PC1) and 34.6% (PC2) of variance (Figure 3). As was the case in the EGC and on the NE Greenland Shelf, dissolved Mn, dCo and dCu in the Barents Sea Opening were grouped opposite to salinity suggesting their distribution was strongly influenced by sources associated with low salinity waters. Macronutrients across the Barents Sea Opening were positively correlated with salinity and aligned closely with depth, suggesting remineralization as the main driver controlling their distributions. In between these two groupings, dissolved Fe, dNi and dZn across the Barents Sea Opening were aligned suggesting that their distributions are influenced by a mixture of factors including biological activity and the associated remineralization, with low salinity waters being a minor controlling factor.

3.2. Micronutrient Sources to Fram Strait

Macronutrient and micronutrient distributions in Fram Strait are strongly influenced by North Atlantic and Arctic waters (Krisch et al., 2020; Torres-Valdés et al., 2013). Atlantic Water that forms the core of the WSC (Beszczynska-Möller et al., 2012; Rudels, 2019) showed 0.67 ± 0.32 nM dFe, 1.11 ± 0.26 nM dMn, 86 ± 13 pM dCo, 3.27 ± 0.11 nM dNi and 1.30 ± 0.08 nM dCu in Fram Strait, matching observations of Atlantic Water in the Barents Sea Opening (Table S3 in Supporting Information S1). Dissolved Zn was ~3-fold elevated in Atlantic Water of the WSC (2.06 ± 1.10 nM) compared to concentrations in the Barents Sea Opening (0.74 ± 0.23 nM), but showed only minor enrichment relative to measurements of Atlantic Water in the upstream Iceland and Irminger Basins (1.53 ± 0.45 nM at 80–3,100 m for all stations 20–35°W, Achterberg et al., 2021). Atlantic Water in the Barents Sea Opening is primarily derived from the Norwegian Atlantic Slope Current, whilst the WSC of Fram Strait also comprises Atlantic Water from the North Atlantic Front Current flowing through the central Nordic Seas (Mauritzen et al., 2011; Figure 1). Water column dZn enrichment in the WSC but not the Barents Sea Opening, may thus arise from differences in biological uptake (Kohly, 1998; Vernet et al., 2019) and water mass mixing (Middag et al., 2019; Roshan & Wu, 2015) between these two Atlantic Water source regions.

Dissolved Fe in Atlantic Waters of the Fram Strait (0.80 ± 0.37 nM for all stations) and Barents Sea Opening (0.59 ± 0.33 nM) showed typical concentrations for the North Atlantic and was comparable to observations from Atlantic Water in both the upstream Iceland and Irminger Basins (0.66 ± 0.41 nM at 80–3,100 m for all stations 20–35°W, Achterberg et al., 2018), and the downstream SE Nansen Basin (0.70 ± 0.25 nM at stations 239–260 as per Klunder, Laan, et al., 2012). Similarly, dissolved Co, Ni and Cu in Atlantic Water from Fram Strait and the Barents Sea Opening (Table S3 in Supporting Information S1) matched observations in the Iceland and Irminger Basins (87 ± 20 pM dCo, 3.90 ± 0.52 nM dNi, 1.25 ± 0.08 nM dCu, Achterberg et al., 2021). Dissolved Mn on the other hand was ~2-fold elevated in Atlantic Water at Fram Strait (0.96 ± 0.32 nM) relative to observations from Atlantic Water in the Iceland and Irminger Basins (0.50 ± 0.37 nM, Achterberg et al., 2021). This suggests that during northward transport in the high latitude North Atlantic and across the Nordic Seas, sources and sinks of dFe, dCo, dNi and dCu are roughly balanced, whereas other micronutrients such as dMn and dZn are subject to ongoing net inputs, for example, from Svalbard shelf sediments (Gerringa, Rijkenberg, et al., 2021), before entering the Arctic Ocean.

Dissolved micronutrient concentrations in the water column of the EGC were higher than any other water mass beyond the NE Greenland shelf break and showed greater spatial variability, except for dZn (Table S3 in Supporting Information S1). While dMn, dCo and dNi showed similar concentrations in the EGC in Fram Strait (0.78 ± 0.76 nM dMn, 81 ± 25 pM dCo and 3.56 ± 0.58 nM dNi for all stations between 2°E−6.5°W) to those observed in the EGC in Southeast Greenland (0.80 ± 0.40 nM dMn, 94 ± 34 pM dCo and 3.72 ± 0.66 nM dNi at 60°N, 41–43°W, Achterberg et al., 2021), average concentrations of dFe (0.85 ± 0.45 nM), dCu (1.67 ± 0.59 nM) and dZn (2.16 ± 1.10 nM) were ~30%–50% elevated in the EGC in Fram Strait compared to concentrations in the EGC further south (0.54 ± 0.27 nM dFe, 1.32 ± 0.17 nM dCu and 1.46 ± 1.55 nM dZn, Achterberg et al., 2021). This apparent loss of dFe, dCu and dZn in the EGC between Fram Strait and Southeast Greenland may be linked to phytoplankton uptake (Morel et al., 2003), scavenging of dFe (Bruland et al., 2013), and incorporation of ambient low dFe, low dCu and low dZn waters (Achterberg et al., 2018, 2021) sufficient enough to more than offset any new input of these elements from the Greenland shelf.

Whilst this comparison refers to data from different years (2010 and 2016), the apparent north-south gradient in summertime (July–August) dissolved micronutrient concentrations extends further north when considering observations in the Central Arctic Ocean as of 2015. Near the North Pole, concentrations of dFe (2.28 ± 0.96 nM), dMn (3.66 ± 1.43 nM), dCo (145 ± 31 pM), dNi (7.13 ± 1.07 nM) and dCu (5.79 ± 1.30 nM) are even more elevated in the Transpolar Drift. The Transpolar Drift holds a fraction of up to 25% meteoric freshwater and is rich in shelf-derived material (Charette et al., 2020; Kipp et al., 2018; Rutgers van der Loeff et al., 2018), including organic material that stabilizes concentrations of micronutrients such as dFe several factors beyond the capacity of ambient seawater via complexation (e.g., 2.5–4.4 nM dFe inside the Transpolar Drift compared to ~0.6 nM outside the Transpolar Drift) (Klunder, Bauch, et al., 2012; Rijkenberg et al., 2018; Slagter et al., 2017). Ligand stabilization may similarly cause elevated concentrations of other organically complexed micronutrients including dCo, dNi and dCu (Bundy et al., 2020; Charette et al., 2020). The Transpolar Drift is advected toward Fram Strait (Krumpen et al., 2019; Mysak, 2001), and so Arctic Ocean surface waters, likely including smaller fractions of Pacific Water (Aksenov et al., 2016; Dmitrenko et al., 2019), contribute to the EGC (Laukert et al., 2017; Richter et al., 2018; Rudels, 2019) and appear to function as a source of elevated dissolved micronutrient concentrations to the high latitude North Atlantic.

Although glacial discharge is likely the source of observed dFe, dMn, dCo, dNi and dCu maxima near coastal Greenland (stations 20–22, Figure 2; Krause et al., 2021; Krisch, Hopwood, et al., 2021), Greenland Ice Sheet discharge is unlikely a substantial contributor to the EGC beyond the shelf break (Huhn et al., 2021; Laukert et al., 2017). Efficient estuarine removal, particularly of dFe (Krause et al., 2021; Zhang et al., 2015), and the limited potential to stabilize additional quantities of ligand-bound micronutrients (Ardiningsih et al., 2020; Krisch, Hopwood, et al., 2021) are major constraints on Greenland Ice Sheet micronutrient export. Concentrations in the surface EGC at 78°50'N (0.56 ± 0.14 nM dFe, 0.96 ± 0.30 nM dMn, 85 ± 28 pM dCo, 3.19 ± 0.22 nM dNi and 1.45 ± 0.32 nM dCu for <500 m at stations 14, 15 and 26) were similar to observations in Atlantic Water of the WSC. This suggests a minor influence of glacial discharge, but recirculation in Fram Strait (de Steur et al., 2014; Hattermann et al., 2016) may exert a strong control on micronutrient distributions in the western parts of Fram Strait (Figure S2 in Supporting Information S1).

Further north, the water column of EGC stations 8, 9 and 25 (79.6–80.9°N) revealed similar trends in the distribution of dFe, dMn, dCo, dNi and dCu to stations in the Transpolar Drift from the surface to ~1500 m depth (Figure S5 in Supporting Information S1). Concentrations of dFe, dMn, dCo, dNi and dCu measured in Surface Water of the EGC (stations 8, 9 and 25) were however at the lower end of observations in the Transpolar Drift suggesting progressive dilution/loss of dissolved micronutrients as the current progresses southwards across the Arctic (Aagaard & Carmack, 1989; Charette et al., 2020; Smedsrud et al., 2017). Additionally, there may have been mixing with micronutrient-depleted Polar Surface Water (Gerringa, Rijkenberg, et al., 2021) and Recirculating Atlantic Water (Krisch et al., 2020) to the north of Fram Strait (Hattermann et al., 2016; Laukert et al., 2017; Richter et al., 2018). Below 1500 m, concentrations of dFe, dMn and dCo in the EGC increased with depth and contrast to stations in the Transpolar Drift where their distribution evidenced little variation between 1500 m and 3,500 m likely a consequence of the lack of micronutrient input and enhanced scavenging in the Central Arctic Ocean (Gerringa, Rijkenberg, et al., 2021; Valk et al., 2018). Dissolved Zn showed a contrasting behavior and was neither enriched in the Transpolar Drift (1.61 ± 0.77 nM) nor in EGC Surface Water at stations 8, 9 and 25 (1.38 ± 0.54 nM). Other trace elements from the same expeditions such as mercury ("total Hg', Charette et al., 2020; Petrova et al., 2020) corroborate our conclusion of Arctic Ocean surface waters being a source of trace elements to Fram Strait and the North Atlantic Ocean by advection with the Transpolar Drift and into East Greenland Current.

3.3. Siberian Shelf Sources

If the Transpolar Drift acts as a source of Arctic Ocean shelf-derived micronutrients to the North Atlantic, dissolved Fe, dMn, dCo, dNi and dCu enrichment in Fram Strait should show a correlation with meteoric freshwater and ligand content similar to observations in the Central Arctic Ocean. For the calculation of meteoric freshwater contents, we use oxygen isotope measurements ($\delta^{18}O$) from GN05 (Meyer et al., 2021) with a freshwater reference $\delta^{18}O$ value of −20‰ which is an average for riverine discharge to the Arctic Ocean shelves (Bauch et al., 2011; Dubinina et al., 2017). The $\delta^{18}O$ measurements reveal an east-to-west gradient of meteoric freshwater contents in surface waters of Fram Strait (Figure S6 in Supporting Information S1). Minima were calculated for the surface WSC (~0% at <50 m between 7.0 and 8.6°E), which is consistent with prior surface $\delta^{18}O$ measurements (+0.2 ± 0.1‰ at <50 m) and corresponding meteoric freshwater contents (~0%) in the upstream Norwegian and Greenland Sea (65–75°N, 10°E−10°W; Schmidt et al., 1999). The surface EGC showed pronounced maxima in meteoric freshwater (14 ± 3% in the water column <50 m at 80°N, 4.0–8.2°W) comparable to the lower end of observations in the Central Arctic Ocean near the North Pole (20 ± 4% at >88°N; Pasqualini et al., 2017).

Plotting micronutrient concentrations against meteoric freshwater content (Figure S7 in Supporting Information S1) shows increasing concentrations of dMn (R^2 0.45), dCo (R^2 0.73), dNi (R^2 0.78) and dCu (R^2 0.88) at elevated freshwater contents in the water column of Fram Strait. The regression coefficients are comparable to observations in the Central Arctic Ocean Transpolar Drift (R^2 0.41 for dMn, R^2 0.54 for dCo, R^2 0.91 for dNi and R^2 0.96 for dCu as per Charette et al., 2020). Micronutrient freshwater endmembers in Fram Strait, calculated from extrapolation of the linear fit to 100% meteoric freshwater, are similar to freshwater endmembers of the Transpolar Drift (Table S4 in Supporting Information S1). This suggests little change in the efficiency of dMn, dCo, dNi and dCu transport as the Transpolar Drift transits across the Arctic and through Fram Strait. The correlation of dFe against meteoric freshwater content was, however, much less pronounced in Fram Strait (R^2 0.21) than in the Transpolar Drift (R^2 0.67, Charette et al., 2020) with a corresponding dFe freshwater endmember that was ~4-fold depleted in Fram Strait (4.3 nM) compared to the Central Arctic Ocean (19.3 nM). This may be a consequence of sedimentary dFe enrichment to saline waters (Figure 2) and glacial discharge to the NE Greenland Shelf that shows a distinctly different dFe-salinity relationship compared to waters in the Central Arctic Ocean (Charette et al., 2020; Krisch, Hopwood, et al., 2021). As is the case in the Transpolar Drift, low salinity waters in the EGC were enriched in dFe-binding ligands (1.9 ± 0.6 equivalent nM dFe at <75 m) relative to ligand concentrations in saline Atlantic and Upper Atlantic Water of the WSC (1.2 ± 0.2 equivalent nM Fe) (Ardiningsih et al., 2020; Slagter et al., 2017). Together with dFe, dMn, dCo, dNi and dCu maxima, this suggests a strong influence of Arctic Ocean shelf-derived material on the distribution of dissolved micronutrients in the western Fram Strait.

The flow path of micronutrient transport from the Siberian shelf via the Transpolar Drift to Fram Strait can also be traced through the use of radium (Ra). Ra is released from shelf sediments through continuous decay of

thorium (^{230}Th and ^{232}Th) (Kipp et al., 2018; Rutgers van der Loeff et al., 1995). While thorium is particle-reactive and largely immobilized on lithogenic material (Santschi et al., 2006; Trimble et al., 2004), ^{228}Ra (half-life of 5.75 years) and ^{226}Ra (half-life of 1600 years) are soluble in seawater and, after release, advected with the prevailing currents across the Arctic Ocean (Kipp et al., 2018, 2019; Rutgers van der Loeff et al., 2018). In 2015, activity ratios of ^{228}Ra/^{226}Ra (1.0 ± 0.7 at >85°N) showed a close relationship with meteoric freshwater content (0.077 S, R^2 0.91, Figure S8 in Supporting Information S1) in the upper 500 m of the Central Arctic Ocean (Charette et al., 2020), pointing toward riverine discharge and shelf sediments as strong sources of ^{228}Ra to the region near the North Pole (Kipp et al., 2018; Rutgers van der Loeff et al., 2018). The water column of Fram Strait as of 2016, and the EGC more specifically, showed a similar relationship between ^{228}Ra/^{226}Ra and meteoric freshwater content, although with a less pronounced slope (0.031 S, 0.81 R^2 for all stations in Fram Strait; 0.039 S, 0.97 R^2 in the EGC; Figure S8 in Supporting Information S1), implying that compared to observations in the Central Arctic Ocean, ^{228}Ra in Fram Strait was ~2-fold depleted relative to ^{226}Ra. On the Northeast Greenland Shelf both the meteoric freshwater content and the ^{228}Ra activity are enhanced by local sources (Krisch, Hopwood, et al., 2021), but for the EGC beyond the shelf break such a local source is unlikely to be a major influence (Huhn et al., 2021; Laukert et al., 2017). We explain the reduction in ^{228}Ra/^{226}Ra as the result of radioactive decay of ^{228}Ra during transit from the Siberian shelves to Fram Strait, which can in part occur during the residence of surface waters in the Canada Basin (Kipp et al., 2019). Using Ra as tracer, the timescale of Polar Surface Water advection from the Laptev Sea to the Central Arctic Ocean has been estimated to range between 0.5 and 3 years (Kipp et al., 2018; Rutgers Van Der Loeff et al., 2012). From ^{129}I and ^{236}U measurements (Casacuberta et al., 2018; Wefing et al., 2019) we may infer a further 2–2.5 years for surface waters of the Central Arctic Ocean to reach Fram Strait. This suggests that (micronutrient) trace elements supplied from the Siberian Shelf may reach the ~3,000 km-distant Nordic Seas within 3–5 years. With ^{226}Ra decay being a neglectable source of uncertainty on these times scales, a total transit time on the order of the ^{228}Ra half-life is roughly consistent with the observed decrease in activity.

3.4. Arctic-Atlantic Flux Estimates

In the following, we will discuss dFe, dMn, dCo, dNi, dCu and dZn transport rates ("fluxes") across Fram Strait for August 2016. By the definitions applied herein, negative values indicate Arctic transport toward the North Atlantic Ocean, while positive values indicate transport from the North Atlantic to the Arctic Ocean.

Observations of volume fluxes in August 2006 across Fram Strait suggest transport of North Atlantic-derived micronutrients to the Arctic Ocean as part of the WSC and waters on the NE Greenland Shelf (Tsubouchi et al., 2018). The volume fluxes suggest transport of Arctic Ocean-derived micronutrients toward the North Atlantic as part of the EGC and waters of the Middle section in the deeper parts of Fram Strait (between 6.5°W and 5°E). The northbound WSC and southbound EGC are the dominant water masses by both volume and dissolved micronutrient transport. Together, the WSC and EGC constitute ~80% of gross northbound and southbound dissolved micronutrient fluxes across Fram Strait (Table S5 in Supporting Information S1). Atlantic Water advected from the Nordic Seas (Mauritzen et al., 2011) is the dominant component in the WSC and comprises ~50% of dFe, dCo, dNi and dCu, and ~70% of dMn transport, a consequence of the large volume transport in this layer (~3.4 Sv, Table S5 in Supporting Information S1). Deep Water forms the most dZn enriched water mass and contributes the largest fraction to WSC dZn transport (~45%). Dissolved micronutrient transport in the EGC is different to transport in the WSC as the main transport of dFe, dCo, dNi, dCu and dZn occurs via Intermediate and Deep Water, that originates from the Arctic Ocean (Laukert et al., 2017; Meincke et al., 1997). Intermediate Water dominates southbound dissolved micronutrient transport and comprises ~35% of gross dFe, dCo, dNi and dCu fluxes, and ~50% of gross dZn fluxes across Fram Strait. In contrast, major southbound transport of dMn occurs in the surface layer (~40%).

The NE Greenland Shelf, is an additional, yet minor source of dFe, dMn, dCo, dNi, dCu and dZn in Fram Strait and contributed ~10% to gross fluxes (northbound and southbound) across Fram Strait (Table S5 in Supporting Information S1). Dissolved Fe, Mn, Co, Ni and Cu fluxes on the shelf are comparable in magnitude to Arctic export in the EGC Surface Water, and are a factor of 3–5x smaller with respect to the EGC as a whole. However, the shelf region and the EGC are both influenced by sources in the Arctic Ocean (Krisch et al., 2020; Laukert et al., 2017; Michel et al., 2015). Due to the lack of moored instruments measuring volume fluxes in Surface Water near the continental shelf break (Tsubouchi et al., 2018), it is currently impossible to quantify the sole

contribution of Arctic Ocean outflow to dissolved micronutrient fluxes on the NE Greenland Shelf. For August 2016, positive volume fluxes were computed for Surface Water, Upper Atlantic Water and Atlantic Water and suggest net transport of NE Greenland Shelf waters to the Arctic Ocean. Water mass movement on the NE Greenland Shelf is however dominated by an anticyclonic circulation (Bourke et al., 1987). The EGC forms the eastern limb of this shelf circulation (Jeansson et al., 2008), and thus, although the net observable circulation on the NE Greenland Shelf might be directed to the north during times of the year, contributions from shelf sources to dissolved micronutrient fluxes across Fram Strait are likely incorporated into the southward-directed flow field in western Fram Strait (Figure 1).

Shelf processes that affect fluxes on the NE Greenland Shelf are Greenland Ice Sheet discharge and sedimentary release of micronutrients such as dFe and dMn (Krause et al., 2021; Krisch, Hopwood, et al., 2021). We estimated the glacial micronutrient supply from Nioghalvfjerdsbrae to Fram Strait (Table S6 in Supporting Information S1) following the approach outlined in Krisch, Hopwood, et al. (2021), using the mean cavity volume overturning rate (46 ± 11 mSv, Schaffer et al., 2020) and the difference in dissolved micronutrient load between station 19 (cavity-entering Atlantic Intermediate Water) and station 22 (cavity-exiting, glacially modified Atlantic Intermediate Water). We assume, surface runoff is neglectable compared to subglacial discharge, which in the specific case of the glacier Nioghalvfjerdsbrae is likely correct as subglacial melting accounts for >80% of the annual non-calving mass loss (Wilson et al., 2017). This approach suggests glacial discharge from Nioghalvfjerdsbrae to the NE Greenland Shelf of 56 ± 37 $Mg{\cdot}a^{-1}$ dFe, 70 ± 85 $Mg{\cdot}a^{-1}$ dMn, 4.9 ± 4.7 $Mg{\cdot}a^{-1}$ dCo, 6.2 ± 31 $Mg{\cdot}a^{-1}$ dNi and 72 ± 104 $Mg{\cdot}a^{-1}$ dCu. Glacial dZn enrichment in waters downstream the marine terminus was not observed. Nioghavfjerdsbrae, as the largest contributor of freshwater onto the shelf, draining ∼6% of the Greenland Ice Sheet (Rignot & Mouginot, 2012), contributes <2% to southbound dissolved micronutrient transport across the strait suggesting a relatively minor role for glacial discharge to Arctic export in general.

The WSC and EGC were the dominant water masses for dFe, dMn, dCo, dNi, dCu and dZn transport across Fram Strait between September 2005 and August 2006 (Figure 4). Our calculations from micronutrient data as of late summer 2016 applied to monthly variation in volume fluxes from September 2005 and August 2006 suggest Atlantic-derived dFe, dMn, dCo, dNi and dCu transport to the Arctic Ocean as part of the WSC is approximately counter-balanced by Arctic transport toward the North Atlantic Ocean in the EGC between June and February (Tables S7 and S8 in Supporting Information S1). With contributions from the Middle section and the NE Greenland Shelf, there is a net southward transport through Fram Strait of Arctic-sourced dFe (2.3 ± 1.7 $Gg{\cdot}a^{-1}$), dNi (10.1 ± 7.8 $Gg{\cdot}a^{-1}$) and dCu (9.7 ± 4.4 $Gg{\cdot}a^{-1}$), and possibly dMn (1.7 ± 2.0 $Gg{\cdot}a^{-1}$) and dCo (186 ± 202 $Mg{\cdot}a^{-1}$) (Table 2). Monthly mean net exchange rates across Fram Strait show a seasonal trend with maxima in Arctic export in late summer (September) and winter (January–March). Conversely, net northbound transport to the Arctic Ocean was calculated for May (dFe, dMn, dCo and dNi) and August (dMn and dCo), possibly related to the seasonal variability in recirculation and southbound freshwater transport across Fram Strait (de Steur et al., 2009, 2014; Hattermann et al., 2016). As a consequence of the dominance of dZn fluxes in the WSC over the EGC, a net northward flux, but within uncertainty, of 4.9 ± 6.2 $Gg{\cdot}a^{-1}$ dZn to the Arctic Ocean has been calculated. Net fluxes suggest maxima in dZn transport to the Arctic Ocean in spring (April–May), late summer (August) and winter (December), and contrast with September where a pronounced maximum of transport from the Arctic Ocean toward the North Atlantic Ocean is suggested.

Net southbound transport of Arctic dFe, dNi and dCu across Fram Strait is within uncertainty compared to estimates of dissolved micronutrient fluxes in the Transpolar Drift (5.6 ± 2.8 $Gg{\cdot}a^{-1}$ dFe, 14.1 ± 7.0 $Gg{\cdot}a^{-1}$ dNi and 12.7 ± 6.3 $Gg{\cdot}a^{-1}$ dCu as per Charette et al., 2020), and corresponds to ∼1.6% of global riverine dFe (∼140 $Gg{\cdot}a^{-1}$, Raiswell & Canfield, 2012), ∼48% of global riverine dNi (∼21 $Gg{\cdot}a^{-1}$,Cameron & Vance, 2014) and ∼22% of global riverine dCu (∼45 $Gg{\cdot}a^{-1}$,Vance et al., 2008) discharge to the ocean (Table S9 in Supporting Information S1). Whilst southbound transport of Arctic dFe across Fram Strait (2.3 ± 1.7 $Gg{\cdot}a^{-1}$) is only a modest fraction of the transport rates of dFe in the Lena, Ob and Yenisey Rivers (∼30–50 $Gg{\cdot}a^{-1}$, Table S9 in Supporting Information S1), this is not surprising considering the efficient estuarine removal of riverine dFe on the Siberian Shelf (Conrad et al., 2019; Guieu et al., 1996). In contrast, net southbound transport of Arctic dNi and dCu across Fram Strait is ∼5-10-fold greater than the combined riverine supply by the Lena, Ob and Yenisey which may be related to the addition from smaller rivers (Guay et al., 2010) and sedimentary release in Siberian Shelf regions (Guieu et al., 1996). Advected with the Transpolar Drift toward the North Atlantic Ocean, southbound Arctic dFe

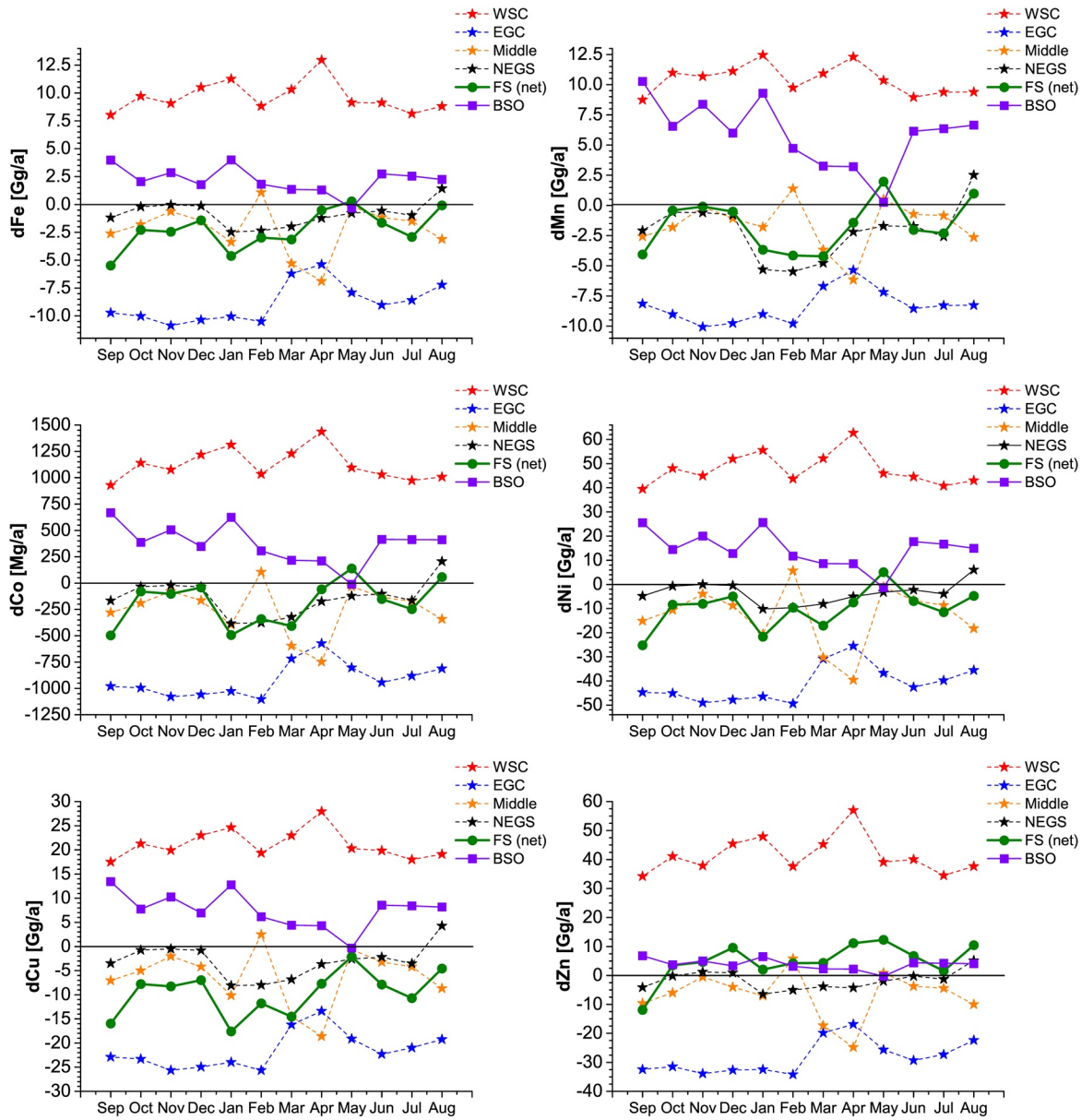

Figure 4. Monthly mean estimates of dFe (top left), dMn (top right), dCo (central left), dNi (central right), dCu (bottom left) and dZn (bottom right) fluxes as part of the (a) West Spitsbergen Current (WSC), (b) East Greenland Current (EGC), (c) "Middle" section, (d) NE Greenland Shelf of FS, and the Barents Sea Branch in the Barents Sea Opening (BSO). Negative (positive) values indicate Arctic export to (import from) the Nordic Seas and the North Atlantic Ocean. Visualized from Tables S7 and S8 in Supporting Information S1.

transport in EGC Surface Water (1.4 ± 1.0 Gg·a^{-1}) may be comparable in magnitude to Greenland ice sheet-to-ocean dFe export (1.6 Gg·a^{-1} as per Krause et al., 2021).

Analogous to Fram Strait, we have calculated dissolved micronutrient fluxes through the Barents Sea Opening (Table 2, Tables S7 and S8 in Supporting Information S1). A detailed report concerning micronutrient cycling in the Barents Sea Opening has been conducted by Gerringa, Rijkenberg, et al. (2021). Our data indicate a net transport of dissolved micronutrients from the Atlantic to the Arctic Ocean through the Barents Sea Opening throughout the year (Figure 4). Atlantic Water was the dominant component and contributed ~50% of this net flux for dFe, dNi, dCu and dZn transport, whereas Surface and Upper Atlantic Water were the main components for dMn (~65%) and dCo (~60%). As observed for Fram Strait, a seasonal trend in dissolved micronutrient transport across the Barents Sea Opening based on volume transport rates is evident. Most prominently, dissolved

Table 2
Annual Net Arctic-Atlantic Dissolved Micronutrient Fluxes Across Fram Strait, the Barents Sea Opening, and Davis Strait

	dFe [Gg a^{-1}]	dMn [Gg a^{-1}]	dCo [Mg a^{-1}]	dNi [Gg a^{-1}]	dCu [Gg a^{-1}]	dZn [Gg a^{-1}]
Fram Strait	−2.3 ± 1.7	−1.7 ± 2.0	−186 ± 202	−10.1 ± 7.8	−9.7 ± 4.4	4.9 ± 6.2
Barents Sea Opening	2.2 ± 1.1	5.9 ± 2.7	374 ± 177	14.6 ± 7.2	7.6 ± 3.6	3.8 ± 1.8
Davis Strait[a]	−2.6 ± 1.3	−7.0 ± 3.3	−461 ± 147	−19.5 ± 6.7	−12.1 ± 3.9	−5.7 ± 3.5
Net Flux	**−2.7 ± 2.4**	**−2.8 ± 4.7**	**−273 ± 306**	**−15.0 ± 12.5**	**−14.2 ± 6.9**	**3.0 ± 7.3**

Note. Negative (positive) values indicate Arctic export to (import from) the Nordic Seas and the North Atlantic Ocean. Mean value of monthly net micronutrient fluxes ± standard deviation (1σ) of monthly variations (September 2005–August 2006).
[a]Calculation of Davis Strait micronutrient export conducted from the annual mean net volume flux across Davis Strait (±1σ) and dissolved concentrations in components of Baffin Bay stations BB1 and BB3 (±1σ) (Colombo et al., 2020). Uncertainty derived from error propagation including the standard deviation in volume fluxes and the standard deviation of observed dFe, dMn, dNi, dCu, dZn and labile dCo concentrations.

micronutrient fluxes through the Barents Sea Opening mirrored net transport rates of Fram Strait (Figure 4). This was most evident in May, when the balancing of dissolved micronutrient fluxes across the Barents Sea Opening coincided with stagnating Arctic export through the Fram Strait "Middle" section (2–5°E) and decreased dFe, dMn, dCo, dNi, dCu and dZn transport in the WSC.

Contributions to Arctic-Atlantic dissolved micronutrient exchange were also calculated for Davis Strait for comparison. Because monthly mean volume fluxes and trace element data are not available, calculations for Davis Strait differ from the micronutrient flux calculations of the Fram Strait and Barents Sea Opening. A detailed investigation concerning micronutrient cycling and fluxes across Davis Strait will follow elsewhere. We apply annual mean net volume fluxes in water layers of Davis Strait (Tsubouchi et al., 2018) to dissolved micronutrient data from two stations sampled in Baffin Bay (part of GEOTRACES expedition GN02, August 2015) (Table S10 in Supporting Information S1). These stations (BB1, BB3) have been analyzed, excluding a UV-digestion step, for dFe, dMn, dNi, dCu, dZn, and the labile fraction of dCo ("labile dCo") referring to weakly complexed and inorganic dCo (e.g., Saito & Moffett, 2001). Stations BB1 and BB3 are affected by the southbound Baffin Current and are thus representative for Arctic micronutrient export across Davis Strait (Colombo et al., 2020). Our calculations suggest Davis Strait is an additional gateway for transport of dFe, dMn, labile dCo, dNi, dCu and dZn from the Arctic to the North Atlantic Ocean (Table 2). Surface Water, including contributions from freshwater and sediment sources in the Canadian Arctic Archipelago (Colombo et al., 2020, 2021), was the dominant component in the water column and comprised ∼80% of dFe, ∼94% of dMn, ∼85% of dCo, dNi and dCu and ∼74% of dZn fluxes across Davis Strait.

Unfortunately, with missing data on monthly changes in volume fluxes and missing data concerning seasonal change in trace element concentrations, we cannot estimate seasonal trends in Davis Strait dissolved micronutrient fluxes. Also, as a consequence of the lack of trace element data in the eastern part of Davis Strait, it is currently impossible to draw any conclusions on dissolved micronutrient fluxes from the North Atlantic Ocean to Baffin Bay–which includes contributions originating from the EGC (Cossa et al., 2018; Tonnard et al., 2020) that are likely recirculated in the West Greenland Current and into Baffin Bay (Colombo et al., 2020). Based on available data from GEOTRACES cruise GA01 sampling the West Greenland Current entering the Labrador Sea off the southern tip of Greenland, concentrations of dFe, dMn, dCo and dCu in the Baffin Current were almost consistently higher, up to one order of magnitude in the case of dMn, than those observed in the water column of the West Greenland Current, the only notable exception being dFe in Surface Water of the Baffin Current at 150 and 200 m depth (Figure S9 in Supporting Information S1). Consequently, a strong gradient in dissolved micronutrient concentrations between regions influenced by the North Atlantic inflow (along the West Greenland coastline) and Arctic Ocean outflow (coastal Canada) is expected in Davis Strait (Colombo et al., 2019, 2020). Calculating micronutrient fluxes only from concentrations of dFe, dMn, dNi, dCu, dZn and the labile fraction of dCo in the Baffin Current herein likely overestimates Arctic contributions to outflow across Davis Strait. However, it is clear from the limited available data that net southbound transport through Davis Strait may be in the same range as net northbound transport of dFe, dMn, dCo, dNi, dCu and dZn through the Barents Sea Opening (Figure 5).

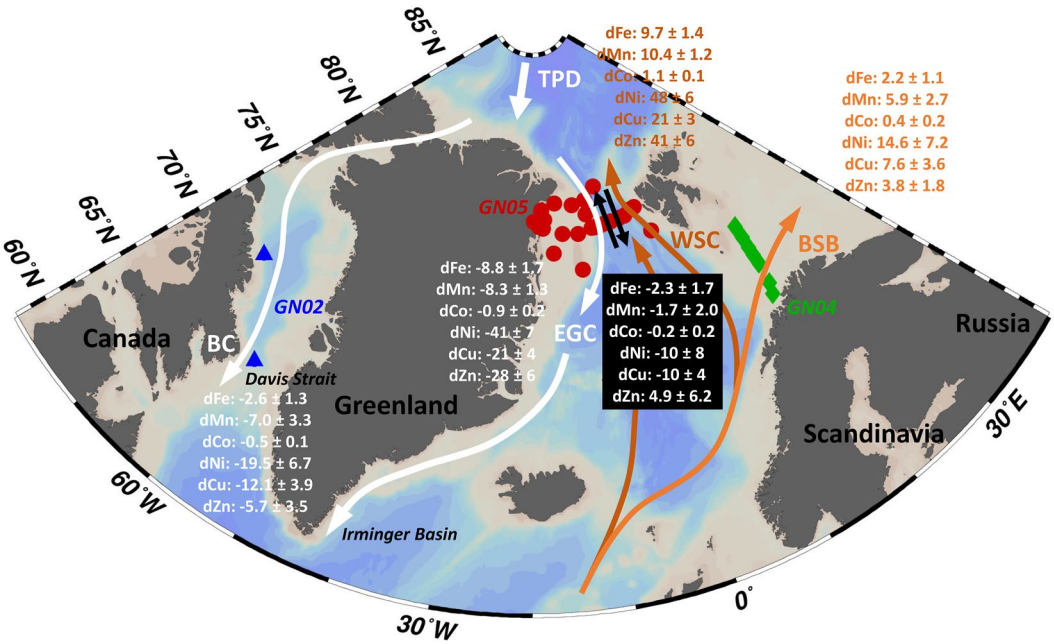

Figure 5. Schematic of annual dFe, dMn, dCo, dNi, dCu and dZn fluxes (in Gg·a^{-1}) in major water masses of Arctic Ocean-high latitude North Atlantic micronutrient transport: The West Spitsbergen Current (WSC), the Barents Sea Branch (BSB), the East Greenland Current (EGC) and the Baffin Current (BC). Black-boxed fluxes refer to the sum of net exchange across Fram Strait and include contributions from the WSC, EGC, the Middle section and fluxes on the NE Greenland Shelf. Positive fluxes (in orange/brown) suggest net import of Atlantic dissolved micronutrients to the Arctic Ocean. Negative fluxes (in white) suggest net export of Arctic dissolved micronutrients to the Nordic Seas and the high latitude North Atlantic. Orange/brown arrows (white arrows) indicate the flow path of warm and saline (cold and fresh) Atlantic waters (Arctic waters). The location of the Transpolar Drift (TPD) is depicted as thick white arrow. Location of stations depicted as red dots (GN05, FS), green diamonds (GN04, Barents Sea Opening) and blue triangles (GN02, Baffin Bay). For WSC, EGC and BSB: Mean value of monthly net micronutrient fluxes ± standard deviation (1σ) of monthly variations (September 2005–August 2006, Tables S7 and S8 in Supporting Information S1). Calculation for Davis Strait conducted from the annual mean net volume flux, and uncertainty derived from error propagation including the standard deviation in annual volume flux and the standard deviation of observed dFe, dMn, labile dCo, dNi, dCu and dZn concentrations.

Micronutrient fluxes from all three gateways combined suggest that there is a net flux of 2.7 ± 2.4 Gg·a^{-1} dFe, 2.8 ± 4.7 Gg·a^{-1} dMn, 273 ± 306 Mg·a^{-1} dCo, 15.0 ± 12.5 Gg·a^{-1} dNi and 14.2 ± 6.9 Gg·a^{-1} dCu from the Arctic toward the North Atlantic Ocean – although the dMn and dCo fluxes calculated remain within uncertainty (Table 2). For dZn, a net northward flux, within uncertainty, of 3.0 ± 7.3 Gg·a^{-1} dZn to the Arctic Ocean has been calculated. The calculated uncertainties in Arctic-Atlantic micronutrient budgets are predominately a consequence of seasonal variability in water flow across Fram Strait. Our data suggests Fram Strait is the most important gateway for Arctic Ocean – North Atlantic Ocean dissolved micronutrient exchange with its importance being a result of gross dFe, dMn, dCo, dNi, dCu and dZn transport in individual water masses (EGC, WSC) rather than from net exchange rates.

3.5. Uncertainty in Micronutrient Fluxes

Estimates of annual micronutrient fluxes across the Arctic Ocean boundaries based on trace element data from August 2015 (Davis Strait, GN02), October 2015 (Barents Sea Opening, GN05) and July–August 2016 (Fram Strait, GN05) are subject to uncertainty concerning seasonal variations in dissolved micronutrient concentrations. Unfortunately, data on seasonal micronutrient concentrations in the Arctic Ocean boundary regions considered herein are lacking. Two sampling campaigns in spring and summer 2010 to the Irminger and Iceland Basins are the only available datasets showing seasonal cycling of dFe, dMn, dCo, dNi, dCu and dZn in the high latitude North Atlantic to date (Achterberg et al., 2018, 2021).

In the Irminger Basin, dissolved Fe, Mn, Co, Ni, Cu and Zn in surface waters are progressively depleted and exported to depth because of primary production in spring and summer, followed by deep winter mixing which resupplies

dissolved micronutrients to surface waters. Dissolved micronutrient concentrations in deeper waters (>500 m) remained fairly constant (Figure S10 in Supporting Information S1) as a consequence of the young age of these waters and an established equilibrium between dissolution and scavenging (Achterberg et al., 2018, 2021). For Fram Strait, the same is to be expected. Intermediate and Deep Water, responsible for ~27% of gross dMn and ~50%–65% of gross dFe, dCo, dNi, dCu and dZn transport through Fram Strait, are young and may show little seasonal variation in dissolved micronutrient concentrations. Thus, interannual variations in Arctic-Atlantic dissolved micronutrient exchange may be primarily driven by seasonal change in volume transport, which is accounted for in our calculations. Yet, superimposed on these processes is the overwhelming influence of southward transport of dFe, dMn, dCo, dNi and dCu from the Central Arctic. Shelf micronutrient supply to the surface Arctic Ocean, including dissolved components from riverine discharge, is seasonally variable (Hölemann et al., 2005; Holmes et al., 2012; Kipp et al., 2018), and seasonal variability is also seen in the formation of the EGC in Fram Strait (de Steur et al., 2014, 2018; Tsubouchi et al., 2018). Likewise, seasonal variability in sea ice dynamics (Smedsrud et al., 2017), glacial discharge (Mankoff et al., 2020), shelf benthic processing, upwelling or downwelling (Schulze & Pickart, 2012; Williams & Carmack, 2015), and the general circulation pattern on the NE Greenland Shelf (Michel et al., 2015) may result in pulses of micronutrient mobilization in surface Fram Strait which are unconstrained to date. Because of data scarcity, it therefore remains challenging to predict when seasonal maxima and minima of dissolved micronutrient transport occur, especially in the surface water masses of western Fram Strait.

4. Conclusion and Future Perspectives

This study represents the first attempt to quantify fluxes of micronutrients between the Arctic and Atlantic Oceans across the gateways of the Fram Strait, Barents Sea Opening and Davis Strait. Our analyses suggest that the Arctic is a net source of dFe, dCo, dNi and dCu, and possibly dMn to the Nordic Seas and to the North Atlantic Ocean. Among the Arctic-Atlantic gateways, Fram Strait is most important for dissolved micronutrient exchange which is a consequence of deep water mass movement (>500 m) across the strait. However, large uncertainties in seasonal changes remain, especially in the western part influenced by the EGC, where dFe, dMn, dCo, dNi and dCu show unusual maxima in surface waters due to pronounced Arctic Ocean export. Data deficiency is presently most problematic in determining fluxes across Davis Strait, which may be comparable in magnitude to those across the Barents Sea Opening. Advection of Arctic and Atlantic Waters to Fram Strait, and recirculation of water masses in Fram Strait, are the major processes controlling dissolved micronutrient availability between Svalbard and NE Greenland. We show that the Transpolar Drift is the most important contributor to transport maxima in surface Fram Strait (<500 m) including waters on the NE Greenland Shelf. This trace element-rich source water has a profound impact on the net flux of Arctic dFe, dMn, dCo, dNi and dCu toward the North Atlantic Ocean. Contributions from the NE Greenland Shelf including glacial discharge to Fram Strait budgets are currently minor. The advection of dissolved micronutrients from the Central Arctic Ocean, including potential contributions from particulates in sea ice (Measures, 1999; Tovar-Sánchez et al., 2010), is thus likely the dominant factor that results in surplus micronutrients compared to phytoplankton demand in Fram Strait (Krisch et al., 2020).

Recent investigations concerning the future of the Transpolar Drift project increasing transport of shelf-derived material (Kipp et al., 2018), including micronutrients, towards Fram Strait (Bundy et al., 2020; Charette et al., 2020) suggesting a potential for increasing Arctic export of dFe, dMn, dCo, dNi and dCu in the future due to a combination of inter-linked effects associated with increased sea ice loss and shelf interaction. Changing sea ice dynamics may be particularly important for future Arctic-Atlantic exchange via Fram Strait because of the multiple micronutrient sources and sinks affected by shifts in sea ice seasonality. The progressive loss of sea ice may further increase export of redox-sensitive micronutrients such as dMn and dCo in response to enhanced photo-dissolution and solubilization processes in the surface ocean (Moffett & Ho, 1996; Sunda & Huntsman, 1994). Although, conversely, increases in Arctic primary production in response to reductions in summertime sea ice cover (Ardyna et al., 2014; Arrigo & van Dijken, 2015) may increase the demand for micronutrients within the Arctic, and also decrease sediment and micronutrient transport associated with advection of sea ice (Marsay et al., 2018; Measures, 1999) towards Fram Strait (Dethleff & Kuhlmann, 2010).

Dissolved micronutrient fluxes to the Arctic Ocean are dominated by advection of the Atlantic WSC. Recirculation of Atlantic waters (de Steur et al., 2014; Hattermann et al., 2016) may thus exert a strong control on the amount of micronutrient import to the Arctic Ocean with possible knock-on effects on phytoplankton productivity in regions downstream of the WSC such as the Nansen Basin (Rijkenberg et al., 2018) where shelf inputs, for

example, through the Transpolar Drift (Gerringa, Rijkenberg, et al., 2021), are lacking. Seasonal and interannual variability in Atlantic Water transport have been observed (Hattermann et al., 2016; Tsubouchi et al., 2021). The associated biogeochemical effects, particularly of long-term alteration in current regimes (De Jong et al., 2012; Tsubouchi et al., 2021), remain challenging to constrain. Yet, projections concerning the future of the WSC suggests an intensification of Atlantic Water supply to the Arctic Ocean (Wang et al., 2020), or "Atlantification", which may result in increased transport of dFe, dMn, dCo, dNi, dCu and dZn to the Arctic Ocean. Long-term observations at the Arctic Ocean boundaries are needed to gain a better understanding of the variability in micronutrient exchange between the Arctic and Atlantic Ocean, and potential impacts on phytoplankton communities and primary production.

Conflict of Interest

The authors declare no conflicts of interest relevant to this study.

Data Availability Statement

All data used throughout this publication is accessible online. Physical oceanography data can be obtained from: https://doi.pangaea.de/10.1594/PANGAEA.859558 (GN04/PS94, Rabe et al., 2016), and https://doi.pangaea.de/10.1594/PANGAEA.871030 (GN05/PS100, Kanzow et al., 2017). Macronutrient data can be obtained from: https://doi.pangaea.de/10.1594/PANGAEA.868396 (GN04/PS94, van Ooijen et al., 2016), and https://doi.pangaea.de/10.1594/PANGAEA.905347 (GN05/PS100, Graeve et al., 2019). Dissolved micronutrient data can be obtained from: https://dataportal.nioz.nl/doi/10.25850/nioz/7b.b.jc (GN04/PS94, Gerringa, Middag, et al., 2021), and https://doi.pangaea.de/10.1594/PANGAEA.933431 (GN05/PS100, Krisch, Roig, et al., 2021). Radium isotope data can be obtained from: https://www.bco-dmo.org/dataset/718440 (GN01/ HLY1502, Charette & Moore, 2021), the supplement to the publication of Rutgers van der Loeff et al. (2018) (GN04), and https://doi.org/10.1594/PANGAEA.936029 and https://doi.org/10.1594/PANGAEA.936027 (GN05, Rutgers van der Loeff et al., 2021a; 2021b). PS100 (GN05) stable oxygen isotope data can be obtained from: https://doi.pangaea.de/10.1594/PANGAEA.927429 (Meyer et al., 2021). GN02 data of dissolved micronutrients and the physical oceanography for stations BB1 and BB3 has been included in the GEOTRACES IDP 2021 (GEOTRACES Intermediate Data Product Group, 2021).

The map of the study area (Figure 1), section plots (Figure 2) and the flux schematic (Figure 5) were made using Ocean Data View software and DIVA gridding calculations (Schlitzer, 2021) and RTopo-2.0.1 bedrock topography (30-arc seconds resolution) (Schaffer et al., 2016). Principle component analyses (Figure 3) were conducted using Minitab statistical software version 19.2020.1 (Minitab Inc., State College, PA, USA). The plot of monthly mean micronutrient fluxes (Figure 4) was plotted using OriginPro version 9.1.0. (OriginLab Corporation, Northampton, MA, USA).

Acknowledgments
The authors thank chief scientists Ursula Schauer (GN04/PS94) and Torsten Kanzow (GN05/PS100), captain Schwarze and the crew of the RV Polarstern, operated by the Alfred Wegener Institute, Helmholtz Centre for Polar and Marine Research (AWI). We are grateful for the help received from Micha Rijkenberg and Patrick Laan (NIOZ) for organisation, sampling and trace element analyses of GN04. Thanks also to Sven Ober (NIOZ) for the operation and maintenance of the PRISTINE sampling system, and Aridane Gonzalez (IUEM) and Michael Staubwasser (University of Cologne) for their assistance in trace element clean sampling during GN04. Many thanks to Janin Schaffer (AWI), Florian Evers (GEOMAR), Eike Köhn (GEOMAR), Nat Wilson (Woods Hole Oceanographic Institution), and Gerd Rohardt (AWI) for CTD handling and processing, and to Nicola Herzberg, Jaw Chuen Yong, Christian Schlosser and Shaomin Chen (all GEOMAR) for assistance during sampling and trace element analyses of GN05. We are grateful to Takamasa Tsubouchi (University of Bergen) for sharing the volume transport data, to Jan van Ooijen (NIOZ), Martin Graeve and Kai-Uwe Ludwichowski (AWI) for macronutrient analyses, and to Dorothea Bauch and Hanno Meyer (AWI) for the analysis of stable oxygen isotopes. S. K. was financed by GEOMAR and the German Research Foundation (DFG award number AC 217/1-1 to E. A.). The Dutch participation was funded by the Netherlands Organization for Scientific Research (NWO contract number 822.01.018 to L.G.). Open access funding enabled and organized by Projekt DEAL.

References

Aagaard, K., & Carmack, E. C. (1989). The role of sea ice and other fresh water in the Arctic circulation. *Journal of Geophysical Research*, *94*(C10), 14485–14498. https://doi.org/10.1029/jc094ic10p14485

Achterberg, E. P., Steigenberger, S., Klar, J. K., Browning, T. J., Marsay, C. M., Painter, S. C., et al. (2021). Trace element Biogeochemistry in the high-latitude North Atlantic Ocean: Seasonal variations and volcanic inputs. *Global Biogeochemical Cycles*, *35*(3), e2020GB006674. https://doi.org/10.1029/2020GB006674

Achterberg, E. P., Steigenberger, S., Marsay, C. M., Lemoigne, F. A. C., Painter, S. C., Baker, A. R., et al. (2018). Iron Biogeochemistry in the high latitude North Atlantic Ocean. *Scientific Reports*, *8*(1), 1283. https://doi.org/10.1038/s41598-018-19472-1

Aksenov, Y., Karcher, M., Proshutinsky, A., Gerdes, R., De Cuevas, B., Golubeva, E., et al. (2016). Arctic pathways of Pacific water: Arctic Ocean model intercomparison experiments. *Journal of Geophysical Research: Oceans*, *121*(1), 27–59. https://doi.org/10.1002/2015JC011299

Amon, R. M. W., Rinehart, A. J., Duan, S., Louchouarn, P., Prokushkin, A., Guggenberger, G., et al. (2012). Dissolved organic matter sources in large Arctic rivers. *Geochimica et Cosmochimica Acta*, *94*, 217–237. https://doi.org/10.1016/j.gca.2012.07.015

Ardiningsih, I., Krisch, S., Lodeiro, P., Reichart, G. J., Achterberg, E. P., Gledhill, M., et al. (2020). Natural Fe-binding organic ligands in Fram Strait and over the northeast Greenland Shelf. *Marine Chemistry*, *224*, 103815. https://doi.org/10.1016/j.marchem.2020.103815

Ardyna, M., Babin, M., Gosselin, M., Devred, E., Rainville, L., & Tremblay, J. É. (2014). Recent Arctic Ocean Sea ice loss triggers novel fall phytoplankton blooms. *Geophysical Research Letters*, *41*(17), 6207–6212. https://doi.org/10.1002/2014GL061047

Arrigo, K. R., & van Dijken, G. L. (2015). Continued increases in Arctic Ocean primary production. *Progress in Oceanography*, *136*, 60–70. https://doi.org/10.1016/j.pocean.2015.05.002

Bauch, D., Hölemann, J., Andersen, N., Dobrotina, E., Nikulina, A., & Kassens, H. (2011). The Arctic Shelf regions as a source of freshwater and brine-enriched waters as revealed from stable oxygen isotopes. *Polarforschung*, *80*(3), 127–140.

Beszczynska-Möller, A., Fahrbach, E., Schauer, U., & Hansen, E. (2012). Variability in Atlantic water temperature and transport at the entrance to the Arctic Ocean, 1997–2010. *ICES Journal of Marine Science*, *69*(5), 852–863. https://doi.org/10.1038/278097a0

Bourke, H., Newton, J. L., Paquette, G., & Tunnicliffe, M. D. (1987). Circulation and water masses of the east Greenland Shelf. *Journal of Geophysical Research*, *92*(C7), 6729–6740. https://doi.org/10.1029/JC092iC07p06729

Brand, L. E., Sunda, W. G., & Guillard, R. R. L. (1986). Reduction of marine phytoplankton reproduction rates by copper and cadmium. *Journal of Experimental Marine Biology and Ecology*, *96*(3), 225–250. https://doi.org/10.1016/0022-0981(86)90205-4

Browning, T. J., Achterberg, E. P., Engel, A., & Mawji, E. (2021). Manganese co-limitation of phytoplankton growth and major nutrient drawdown in the southern ocean. *Nature Communications*, *12*(1), 884. https://doi.org/10.1038/s41467-021-21122-6

Browning, T. J., Achterberg, E. P., Rapp, I., Engel, A., Bertrand, E. M., Tagliabue, A., & Moore, C. M. (2017). Nutrient co-limitation at the boundary of an oceanic gyre. *Nature*, *551*(7679), 242–246. https://doi.org/10.1038/nature24063

Browning, T. J., Al-Hashem, A. A., Hopwood, M. J., Engel, A., Wake, E. D., & Achterberg, E. P. (2020). Nutrient regulation of late spring phytoplankton blooms in the midlatitude North Atlantic. *Limnology & Oceanography*, *65*(6), 1136–1148. https://doi.org/10.1002/lno.11376

Bruland, K. W., Middag, R., & Lohan, M. C. (2013). *Treatise on Geochemistry* (2nd edn, Vol. 8). Elsevier Ltd. Controls of trace metals in Seawater. https://doi.org/10.1016/B978-0-08-095975-7.00602-1

Bruland Research Lab. (2009). *Consensus values for the GEOTRACES 2008 and SAFe reference samples*. Retrieved from https://websites.pmc.ucsc.edu/~kbruland/GeotracesSaFe/kwbGeotracesSaFe.html

Bundy, R. M., Tagliabue, A., Hawco, N. J., Morton, P. L., Twining, B. S., Hatta, M., et al. (2020). Elevated sources of cobalt in the Arctic Ocean. *Biogeosciences*, *17*(19), 4745–4767. https://doi.org/10.5194/bg-17-4745-2020

Cameron, V., & Vance, D. (2014). Heavy nickel isotope compositions in rivers and the oceans. *Geochimica et Cosmochimica Acta*, *128*, 195–211. https://doi.org/10.1016/j.gca.2013.12.007

Casacuberta, N., Christl, M., Vockenhuber, C., Wefing, A. M., Wacker, L., Masqué, P., et al. (2018). Tracing the three Atlantic branches entering the Arctic Ocean with 129I and 236U. *Journal of Geophysical Research: Oceans*, *123*(9), 6909–6921. https://doi.org/10.1029/2018JC014168

Charette, M. A., Kipp, L. E., Jensen, L. T., Dabrowski, J. S., Whitmore, L. M., Fitzsimmons, J. N., et al. (2020). The transpolar drift as a source of riverine and shelf-derived trace elements to the central Arctic Ocean. *Journal of Geophysical Research: Oceans*, *125*(5), e2019JC015920. https://doi.org/10.1029/2019JC015920

Charette, M. A., & Moore, W. S. (2021). Radium and thorium isotopes measured in the western Arctic as part of the 2015 US GEOTRACES Arctic cruise on the USCGC Healy (HLY1502) from August to October 2015. Version 4 [Dataset]. https://doi.org/10.26008/1912/bco-dmo.718440.4

Coale, K. H., & Bruland, K. W. (1988). Copper complexation in the Northeast Pacific. *Limnology & Oceanography*, *33*(5), 1084–1101. https://doi.org/10.4319/lo.1988.33.5.1084

Colombo, M., Jackson, S. L., Cullen, J. T., & Orians, K. J. (2020). Dissolved iron and manganese in the Canadian Arctic Ocean: On the biogeochemical processes controlling their distributions. *Geochimica et Cosmochimica Acta*, *277*, 150–174. https://doi.org/10.1016/j.gca.2020.03.012

Colombo, M., Rogalla, B., Li, J., Allen, S. E., Orians, K. J., & Maldonado, M. T. (2021). Canadian Arctic Archipelago Shelf-Ocean interactions: A major iron Source to Pacific derived waters transiting to the Atlantic. *Global Biogeochemical Cycles*, *35*(10), e2021GB007058. https://doi.org/10.1029/2021GB007058

Colombo, M., Rogalla, B., Myers, P. G., Allen, S. E., & Orians, K. J. (2019). Tracing dissolved lead sources in the Canadian Arctic: Insights from the Canadian GEOTRACES program. *ACS Earth and Space Chemistry*, *3*(7), 1302–1314. https://doi.org/10.1021/acsearthspacechem.9b00083

Conrad, S., Ingri, J., Gelting, J., Nordblad, F., Engström, E., Rodushkin, I., et al. (2019). Distribution of Fe isotopes in particles and colloids in the salinity gradient along the Lena River plume, Laptev Sea. *Biogeosciences*, *16*(6), 1305–1319. https://doi.org/10.5194/bg-16-1305-2019

Cossa, D., Heimbürger, L. E., Pérez, F. F., García-Ibáñez, M. I., Sonke, J. E., Planquette, H., et al. (2018). Mercury distribution and transport in the North Atlantic Ocean along the GEOTRACES-GA01 transect. *Biogeosciences*, *15*(8), 2309–2323. https://doi.org/10.5194/bg-15-2309-2018

Crawford, D. W., Lipsen, M. S., Purdie, D. A., Lohan, M. C., Statham, P. J., Whitney, F. A., et al. (2003). Influence of zinc and iron enrichments on phytoplankton growth in the northeastern Subarctic Pacific. *Limnology & Oceanography*, *48*(4), 1583–1600. https://doi.org/10.4319/lo.2003.48.4.1583

Cutter, G., Casciotti, K., Croot, P., Geibert, W., Heimbürger, L.-E., Lohan, M., et al. (2017). *Sampling and sample-handling protocols for GEOTRACES CruisesGEOTRACES standards and intercalibration committee*. Retrieved from http://www.geotraces.org/science/intercalibration/222-sampling-and-sample-handling-protocols-for-geotraces-cruises

Dai, M. H., & Martin, J. M. (1995). First data on trace metal level and behaviour in two major Arctic River-estuarine systems (Ob and Yenisey) and in the adjacent Kara Sea, Russia. *Earth and Planetary Science Letters*, *131*(3–4), 127–141. https://doi.org/10.1016/0012-821X(95)00021-4

De Jong, M. F., Van Aken, H. M., Våge, K., & Pickart, R. S. (2012). Convective mixing in the central Irminger Sea: 2002-2010. *Deep-Sea Research Part I Oceanographic Research Papers*, *63*, 36–51. https://doi.org/10.1016/j.dsr.2012.01.003

de Steur, L., Hansen, E., Gerdes, R., Karcher, M., Fahrbach, E., & Holfort, J. (2009). Freshwater fluxes in the East Greenland Current: A decade of observations. *Geophysical Research Letters*, *36*(23), L23611. https://doi.org/10.1029/2009GL041278

de Steur, L., Hansen, E., Mauritzen, C., Beszczynska-Möller, A., & Fahrbach, E. (2014). Impact of recirculation on the East Greenland Current in Fram Strait: Results from moored current meter measurements between 1997 and 2009. *Deep-Sea Research Part I Oceanographic Research Papers*, *92*, 26–40. https://doi.org/10.1016/j.dsr.2014.05.018

de Steur, L., Peralta-Ferriz, C., & Pavlova, O. (2018). Freshwater export in the East Greenland current freshens the North Atlantic. *Geophysical Research Letters*, *45*(24), 13359–13366. https://doi.org/10.1029/2018GL080207

Dethleff, D., & Kuhlmann, G. (2010). Fram Strait Sea-ice sediment provinces based on silt and clay compositions identify Siberian Kara and Laptev seas as main source regions. *Polar Research*, *29*(3), 265–282. https://doi.org/10.3402/polar.v29i3.6070

Dmitrenko, I. A., Kirillov, S. A., Rudels, B., Babb, D. G., Myers, P. G., Stedmon, C. A., et al. (2019). Variability of the Pacific-derived Arctic water over the southeastern Wandel Sea Shelf (northeast Greenland) in 2015–2016. *Journal of Geophysical Research: Oceans*, *124*(1), 349–373. https://doi.org/10.1029/2018JC014567

Dubinina, E. O., Kossova, S. A., Miroshnikov, A. Y., & Kokryatskaya, N. M. (2017). Isotope (δD, δ18O) systematics in waters of the Russian Arctic Seas. *Geochemistry International*, *55*(11), 1022–1032. https://doi.org/10.1134/S0016702917110052

Dupont, C. L., Buck, K. N., Palenik, B., & Barbeau, K. (2010). Nickel utilization in phytoplankton assemblages from contrasting oceanic regimes. *Deep-Sea Research Part I Oceanographic Research Papers*, *57*(4), 553–566. https://doi.org/10.1016/j.dsr.2009.12.014

Ezoe, M., Ishita, T., Kinugasa, M., Lai, X., Norisuye, K., & Sohrin, Y. (2004). Distributions of dissolved and acid-dissolvable bioactive trace metals in the North Pacific. *Geochemical Journal*, *38*(6), 535–550. https://doi.org/10.2343/geochemj.38.535

Feng, X., Vonk, J. E., Van Dongen, B. E., Gustafsson, Ö., Semiletov, I. P., Dudarev, O. V., et al. (2013). Differential mobilization of terrestrial carbon pools in Eurasian Arctic River Basins. *Proceedings of the National Academy of Sciences of the United States of America*, *110*(35), 14168–14173. https://doi.org/10.1073/pnas.1307031110

Fu, Y., Feili, L., Karstensen, J., & Wang, C. (2020). A stable Atlantic meridional overturning circulation in a changing North Atlantic Ocean since the 1990s. *Science Advances*, *6*(48), eabc7836. https://doi.org/10.1126/sciadv.abc7836

Garnier, J. M., Martin, J. M., Mouchel, J. M., & Sioud, K. (1996). Partitioning of trace metals between the dissolved and particulate phases and particulate surface reactivity in the Lena River estuary and the Laptev Sea (Russia). *Marine Chemistry*, *53*(3–4), 269–283. https://doi.org/10.1016/0304-4203(95)00094-1

GEOTRACES Intermediate Data Product Group (2021). The GEOTRACES Intermediate Data Product 2021 (IDP2021). NERC EDS British Oceanographic Data Centre NOC. 10.5285/cf2d9ba9-d51d-3b7c-e053-8486abc0f5fd

Gerringa, L., Middag, R., Rijkenberg, M., Slagter, H., Laan, P., Bauch, D., et al. (2021). Dissolved Cd, Co, Cu, Fe, Mn, Ni and Zn in the Arctic Ocean. *NIOZ, V2*. https://doi.org/10.25850/nioz/7b.b.jc

Gerringa, L. J. A., Rijkenberg, M. J. A., Slagter, H. A., Laan, P., Paffrath, R., Bauch, D., et al. (2021). Dissolved Cd, Co, Cu, Fe, Mn, Ni and Zn in the Arctic Ocean. *Journal of Geophysical Research: Oceans*, *126*(9), e2021JC017323. https://doi.org/10.1029/2021jc017323

Graeve, M., Ludwichowski, K.-U., & Krisch, S. (2019). Inorganic nutrients measured on water bottle samples from ultra clean CTD/Water sampler-system during POLARSTERN cruise PS100 (ARK-XXX/2). (version 2) [Dataset]. https://doi.org/10.1594/PANGAEA.905347

Granskog, M. A., Stedmon, C. A., Dodd, P. A., Amon, R. M. W., Pavlov, A. K., Steur, L. D., & Hansen, E. (2012). Characteristics of colored dissolved organic matter (CDOM) in the Arctic outflow in the Fram Strait: Assessing the changes and fate of terrigenous CDOM in the Arctic Ocean. *Journal of Geophysical Research*, *117*(C12), C12021. https://doi.org/10.1029/2012JC008075

Grasshoff, K., Kremlingl, K., & Ehrhardt, M. (1999). *Methods of seawater analysis* (3rd edn). WILEY-VCH Verlag GmbH. https://doi.org/10.1002/9783527613984

Guay, C. K. H., Zhulidov, A. V., Robarts, R. D., Zhulidov, D. A., Gurtovaya, T. Y., Holmes, R. M., & Headley, J. V. (2010). Measurements of Cd, Cu, Pb and Zn in the lower reaches of major Eurasian Arctic Rivers using trace metal clean techniques. *Environmental Pollution*, *158*(2), 624–630. https://doi.org/10.1016/j.envpol.2009.08.039

Guieu, C., Huang, W. W., Martin, J. M., & Yong, Y. Y. (1996). Outflow of trace metals into the Laptev Sea by the Lena River. *Marine Chemistry*, *53*(3–4), 255–267. https://doi.org/10.1016/0304-4203(95)00093-3

Hattermann, T., Isachsen, P. E., Von Appen, W. J., Albretsen, J., & Sundfjord, A. (2016). Eddy-driven recirculation of Atlantic water in Fram Strait. *Geophysical Research Letters*, *43*(7), 3406–3414. https://doi.org/10.1002/2016GL068323

Hölemann, J. A., Schirmacher, M., & Prange, A. (2005). Seasonal variability of trace metals in the Lena River and the southeastern Laptev Sea: Impact of the spring freshet. *Global and Planetary Change*, *48*(1–3), 112–125. https://doi.org/10.1016/j.gloplacha.2004.12.008

Holmes, R. M., McClelland, J. W., Peterson, B. J., Tank, S. E., Bulygina, E., Eglinton, T. I., et al. (2012). Seasonal and annual fluxes of nutrients and organic matter from large rivers to the Arctic Ocean and surrounding seas. *Estuaries and Coasts*, *35*(2), 369–382. https://doi.org/10.1007/s12237-011-9386-6

Huhn, O., Rhein, M., Kanzow, T., Schaffer, J., & Sültenfuß, J. (2021). Submarine meltwater from Nioghalvfjerdsbræ (79 north Glacier), northeast Greenland. *Journal of Geophysical Research: Oceans*, *126*(7), e2021JC017224. https://doi.org/10.1029/2021jc017224

IPCC. (2019). In H.-O., Pörtner, D. C., Roberts, V., Masson-Delmotte, P., Zhai, M., Tignor, E., Poloczanska, et al. (Eds.), *IPCC special report on the ocean and Cryosphere in a changing climate*. Retrieved from https://www.ipcc.ch/srocc/download-report-2/

Jakobsson, M. (2002). Hypsometry and volume of the Arctic Ocean and its constituent seas. *Geochemistry, Geophysics, Geosystems*, *3*(5), 1–18. https://doi.org/10.1029/2001gc000302

Jakobsson, M., Mayer, L., Coakley, B., Dowdeswell, J. A., Forbes, S., Fridman, B., et al. (2012). The international Bathymetric chart of the Arctic Ocean (IBCAO) version 3.0. *Geophysical Research Letters*, *39*(12), L12609. https://doi.org/10.1029/2012GL052219

Jeansson, E., Jutterström, S., Rudels, B., Anderson, L. G., Anders Olsson, K., Jones, E. P., et al. (2008). Sources to the East Greenland current and its contribution to the Denmark Strait overflow. *Progress in Oceanography*, *78*(1), 12–28. https://doi.org/10.1016/j.pocean.2007.08.031

Jensen, L. T., Wyatt, N. J., Twining, B. S., Rauschenberg, S., Landing, W. M., Sherrell, R. M., & Fitzsimmons, J. N. (2019). Biogeochemical cycling of dissolved zinc in the western Arctic (Arctic GEOTRACES GN01). *Global Biogeochemical Cycles*, *33*(3), 343–369. https://doi.org/10.1029/2018GB005975

Kadko, D., Aguilar-Islas, A., Bolt, C., Buck, C. S., Fitzsimmons, J. N., Jensen, L. T., et al. (2019). The residence times of trace elements determined in the surface Arctic Ocean during the 2015 US Arctic GEOTRACES expedition. *Marine Chemistry*, *208*, 56–69. https://doi.org/10.1016/j.marchem.2018.10.011

Kanzow, T. (2017). *Berichte zur Polar und Meeresforschung (Reports on Polar and Marine Research)* (Vol. 705). The expedition PS100 of the research vessel POLARSTERN to the Fram Strait in 2016. https://doi.org/10.2312/BzPM_0705_2017

Kanzow, T., von Appen, W.-J., Schaffer, J., Köhn, E., Tsubouchi, T., Wilson, N., et al. (2017). Physical oceanography measured with ultra clean CTD/Watersampler-system during POLARSTERN cruise PS100. [Dataset]. (ARK-XXX/2). https://doi.org/10.1594/PANGAEA.871030

Kipp, L. E., Charette, M. A., Moore, W. S., Henderson, P. B., & Rigor, I. G. (2018). Increased fluxes of shelf-derived materials to the central Arctic Ocean. *Science Advances*, *4*(1), eaao1302. https://doi.org/10.1126/sciadv.aao1302

Kipp, L. E., Kadko, D. C., Pickart, R. S., Henderson, P. B., Moore, W. S., & Charette, M. A. (2019). Shelf-Basin interactions and water mass residence times in the western Arctic Ocean: Insights provided by radium isotopes. *Journal of Geophysical Research: Oceans*, *124*(5), 3279–3297. https://doi.org/10.1029/2019JC014988

Klunder, M. B., Bauch, D., Laan, P., De Baar, H. J. W., Van Heuven, S., & Ober, S. (2012). Dissolved iron in the Arctic Shelf Seas and surface waters of the central Arctic Ocean: Impact of Arctic River water and ice-melt. *Journal of Geophysical Research*, *117*(C1), C01027. https://doi.org/10.1029/2011JC007133

Klunder, M. B., Laan, P., Middag, R., De Baar, H. J. W., & Bakker, K. (2012). Dissolved iron in the Arctic Ocean: Important role of hydrothermal sources, shelf input and scavenging removal. *Journal of Geophysical Research*, *117*(C4), C04014. https://doi.org/10.1029/2011JC007135

Kohly, A. (1998). Diatom flux and species composition in the Greenland Sea and the Norwegian Sea in 1991–1992. *Marine Geology*, *145*(3–4), 293–312. https://doi.org/10.1016/S0025-3227(97)00115-1

Kondo, Y., Obata, H., Hioki, N., Ooki, A., Nishino, S., Kikuchi, T., & Kuma, K. (2016). Transport of trace metals (Mn, Fe, Ni, Zn and Cd) in the western Arctic Ocean (Chukchi Sea and Canada Basin) in late Summer 2012. *Deep-Sea Research Part I Oceanographic Research Papers*, *116*, 236–252. https://doi.org/10.1016/j.dsr.2016.08.010

Krause, J., Hopwood, M. J., Höfer, J., Krisch, S., Achterberg, E. P., Alarcón, E., et al. (2021). Trace element (Fe, Co, Ni and Cu) dynamics across the salinity gradient in Arctic and Antarctic glacier fjords. *Frontiers of Earth Science*, *9*, 725279. https://doi.org/10.3389/feart.2021.725279

Krisch, S., Browning, T. J., Graeve, M., Ludwichowski, K. U., Lodeiro, P., Hopwood, M. J., et al. (2020). The influence of Arctic Fe and Atlantic fixed N on summertime primary production in Fram Strait, North Greenland Sea. *Scientific Reports*, *10*(1), 15230. https://doi.org/10.1038/s41598-020-72100-9

Krisch, S., Hopwood, M. J., Schaffer, J., Al-Hashem, A. A., Höfer, J., Rutgers van der Loeff, M. M., et al. (2021). The 79°N Glacier cavity modulates subglacial iron export to the NE Greenland Shelf. *Nature Communications*, *12*(1), 3030. https://doi.org/10.1038/s41467-021-23093-0

Krisch, S., Roig, S., Lodeiro, P., Yong, J. C., Herzberg, N., Steffens, T., et al. (2021). Dissolved trace elements (Fe, Mn, Co, Ni, Cu, Zn, Cd and Pb) measured on water bottle samples from ultra clean CTD/Water sampler-system during POLARSTERN cruise PS100/GN05. [Dataset]. (ARK-XXX/2). https://doi.org/10.1594/PANGAEA.933431

Krumpen, T., Belter, H. J., Boetius, A., Damm, E., Haas, C., Hendricks, S., et al. (2019). Arctic warming interrupts the transpolar drift and affects long-range transport of sea ice and ice-rafted matter. *Scientific Reports*, *9*(1), 5459. https://doi.org/10.1038/s41598-019-41456-y

Kwok, R. (2009). Outflow of Arctic Ocean Sea ice into the Greenland and Barent Seas: 1979–2007. *Journal of Climate*, *22*(9), 2438–2457. https://doi.org/10.1175/2008JCLI2819.1

Laufer-Meiser, K., Michaud, A. B., Maisch, M., Byrne, J. M., Kappler, A., Patterson, M. O., et al. (2021). Bioavailable iron produced through benthic cycling in glaciated Arctic fjords (Svalbard). *Nature Communications*, *12*(1), 1349. https://doi.org/10.1038/s41467-021-21558-w

Laukert, G., Frank, M., Bauch, D., Hathorne, E. C., Rabe, B., von Appen, W. J., et al. (2017). Ocean circulation and freshwater pathways in the Arctic Mediterranean based on a combined Nd isotope, REE and oxygen isotope section across Fram Strait. *Geochimica et Cosmochimica Acta*, *202*, 285–309. https://doi.org/10.1016/j.gca.2016.12.028

Lewis, K. M., Van Dijken, G. L., & Arrigo, K. R. (2020). Changes in phytoplankton concentration now drive increased Arctic Ocean primary production. *Science*, *369*(6500), 198–202. https://doi.org/10.1126/science.aay8380

Mankoff, K. D., Noël, B., Fettweis, X., Ahlstrøm, A. P., Colgan, W., Kondo, K., et al. (2020). Greenland liquid water discharge from 1958 through 2019. *Earth System Science Data*, *12*(4), 2811–2841. https://doi.org/10.5194/essd-12-2811-2020

Marsay, C. M., Aguilar-Islas, A., Fitzsimmons, J. N., Hatta, M., Jensen, L. T., John, S. G., et al. (2018). Dissolved and particulate trace elements in late Summer Arctic melt ponds. *Marine Chemistry*, *204*, 70–85. https://doi.org/10.1016/j.marchem.2018.06.002

Mauritzen, C., Hansen, E., Andersson, M., Berx, B., Beszczynska-Möller, A., Burud, I., et al. (2011). Closing the loop - Approaches to monitoring the state of the Arctic Mediterranean during the international polar year 2007–2008. *Progress in Oceanography*, *90*(1–4), 62–89. https://doi.org/10.1016/j.pocean.2011.02.010

Mauritzen, C., Rudels, B., & Toole, J. (2013). The Arctic and Subarctic Oceans/Seas. In G. Siedler, S. M. Griffies, J. Gould, & J. A. Church (Eds.), *Ocean circulation and climate: A 21st Century perspective* (103rd edn, pp. 443–470). https://doi.org/10.1016/B978-0-12-391851-2.00017-9

Measures, C. I. (1999). The role of entrained sediments in sea ice in the distribution of aluminium and iron in the surface waters of the Arctic Ocean. *Marine Chemistry*, *68*(1–2), 59–70. https://doi.org/10.1016/S0304-4203(99)00065-1

Meincke, J., Rudels, B., & Friedrich, H. J. (1997). The Arctic Ocean-Nordic Seas thermohaline system. *ICES Journal of Marine Science*, *54*(3), 283–299. https://doi.org/10.1006/jmsc.1997.0229

Menard, H. W., & Smith, S. M. (1966). Hypsometry of ocean basin provinces. *Journal of Geophysical Research*, *71*(18), 4305–4325. https://doi.org/10.1029/jz071i018p04305

Meyer, H., Schaffer, J., Rabe, B., & Rutgers Van Der Loeff, M. M. (2021). Oxygen and hydrogen isotopes in water samples collected during Polarstern cruise PS100. [Dataset]. https://doi.org/10.1594/PANGAEA.927429

Meyer, H., Schönicke, L., Wand, U., Hubberten, H. W., & Friedrichsen, H. (2000). Isotope studies of hydrogen and oxygen in ground ice—Experiences with the equilibration technique. *Isotopes in Environmental and Health Studies*, *36*(2), 133–149. https://doi.org/10.1080/10256010008032939

Michel, C., Hamilton, J., Hansen, E., Barber, D., Reigstad, M., Iacozza, J., et al. (2015). Arctic Ocean outflow shelves in the changing Arctic: A review and perspectives. *Progress in Oceanography*, *139*, 66–88. https://doi.org/10.1016/j.pocean.2015.08.007

Middag, R., de Baar, H. J. W., & Bruland, K. W. (2019). The relationships between dissolved Zinc and major nutrients phosphate and silicate along the GEOTRACES GA02 transect in the West Atlantic Ocean. *Global Biogeochemical Cycles*, *33*(1), 63–84. https://doi.org/10.1029/2018GB006034

Middag, R., De Baar, H. J. W., Laan, P., & Klunder, M. B. (2011). Fluvial and hydrothermal input of manganese into the Arctic Ocean. *Geochimica et Cosmochimica Acta*, *75*(9), 2393–2408. https://doi.org/10.1016/j.gca.2011.02.011

Moffett, J. W., & Ho, J. (1996). Oxidation of cobalt and manganese in seawater via a common microbially catalyzed pathway. *Geochimica et Cosmochimica Acta*, *60*(18), 3415–3424. https://doi.org/10.1016/0016-7037(96)00176-7

Morel, F. M. M., Milligan, A. J., & Saito, M. A. (2003). Marine bioinorganic chemistry: The role of trace metals in the oceanic cycles of major nutrients. *Treatise on Geochemistry*, *6*, 113–143. https://doi.org/10.1016/B0-08-043751-6/06108-9

Mysak, L. A. (2001). Patterns of Arctic circulation. *Science*, *293*(5533), 1269–1270. https://doi.org/10.1126/science.1064217

Nielsdóttir, M. C., Moore, C. M., Sanders, R., Hinz, D. J., & Achterberg, E. P. (2009). Iron limitation of the postbloom phytoplankton communities in the Iceland Basin. *Global Biogeochemical Cycles*, *23*(3), GB3001. https://doi.org/10.1029/2008GB003410

Panzeca, C., Beck, A. J., Leblanc, K., Taylor, G. T., Hutchins, D. A., & Sañudo-Wilhelmy, S. A. (2008). Potential cobalt limitation of vitamin B12 synthesis in the North Atlantic Ocean. *Global Biogeochemical Cycles*, *22*(2), GB2029. https://doi.org/10.1029/2007GB003124

Pasqualini, A., Schlosser, P., Newton, R., & Koffman, T. N. (2017). U.S. GEOTRACES Arctic section ocean water hydrogen and oxygen stable isotope analyses. Version 1.0. [Dataset]. https://doi.org/10.1594/IEDA/100633

Petrova, M. V., Krisch, S., Lodeiro, P., Valk, O., Dufour, A., Rijkenberg, M. J. A., et al. (2020). Mercury species export from the Arctic to the Atlantic Ocean. *Marine Chemistry*, *225*, 103855. https://doi.org/10.1016/j.marchem.2020.103855

Rabe, B., Schauer, U., Ober, S., Horn, M., Hoppmann, M., Korhonen, M., et al. (2016). Physical oceanography during POLARSTERN cruise PS94 [Dataset]. ARK-XXIX/3. https://doi.org/10.1594/PANGAEA.859558

Raiswell, R., & Canfield, D. E. (2012). The iron bio geochemical cycle past and present. *Geochemical Perspectives*, *1*(1), 1–232. https://doi.org/10.7185/geochempersp.1.1

Randelhoff, A., Holding, J., Janout, M., Sejr, M. K., Babin, M., Tremblay, J. É., & Alkire, M. B. (2020). Pan-Arctic Ocean primary production constrained by turbulent nitrate fluxes. *Frontiers in Marine Science*, *7*, 150. https://doi.org/10.3389/fmars.2020.00150

Rapp, I., Schlosser, C., Rusiecka, D., Gledhill, M., & Achterberg, E. P. (2017). Automated preconcentration of Fe, Zn, Cu, Ni, Cd, Pb, Co, and Mn in seawater with analysis using high-resolution sector field inductively-coupled plasma mass spectrometry. *Analytica Chimica Acta*, *976*, 1–13. https://doi.org/10.1016/j.aca.2017.05.008

Rawlins, M. A., Steele, M., Holland, M. M., Adam, J. C., Cherry, J. E., Francis, J. A., et al. (2010). Analysis of the Arctic system for freshwater cycle intensification: Observations and expectations. *Journal of Climate*, *23*(21), 5715–5737. https://doi.org/10.1175/2010JCLI3421.1

Richter, M. E., Von Appen, W. J., & Wekerle, C. (2018). Does the East Greenland current exist in the northern Fram Strait? *Ocean Science*, *14*(5), 1147–1165. https://doi.org/10.5194/os-14-1147-2018

Ricker, R., Kauker, F., Schweiger, A., Hendricks, S., Zhang, J., & Paul, S. (2021). Evidence for an increasing role of ocean heat in Arctic Winter Sea ice growth. *Journal of Climate*, *34*(13), 5215–5227. https://doi.org/10.1175/JCLI-D-20-0848.1

Rignot, E., & Mouginot, J. (2012). Ice flow in Greenland for the international polar year 2008–2009. *Geophysical Research Letters*, *39*(11), L11501. https://doi.org/10.1029/2012GL051634

Rijkenberg, M. J. A., de Baar, H. J. W., Bakker, K., Gerringa, L. J. A., Keijzer, E., Laan, M., et al. (2015). PRISTINE. A new high volume sampler for ultraclean sampling of trace metals and isotopes. *Marine Chemistry*, *177*, 501–509. https://doi.org/10.1016/j.marchem.2015.07.001

Rijkenberg, M. J. A., Middag, R., Laan, P., Gerringa, L. J. A., Van Aken, H. M., Schoemann, V., et al. (2014). The distribution of dissolved iron in the West Atlantic Ocean. *PLoS One*, *9*(6), e101323. https://doi.org/10.1371/journal.pone.0101323

Rijkenberg, M. J. A., Slagter, H. A., Rutgers Van Der Loeff, M., Ooijen, J. V., & Gerringa, L. J. A. (2018). Dissolved Fe in the deep and upper Arctic Ocean with a focus on Fe limitation in the Nansen Basin. *Frontiers in Marine Science*, *5*, 88. https://doi.org/10.3389/fmars.2018.00088

Roshan, S., & Wu, J. (2015). Water mass mixing: The dominant control on the zinc distribution in the North Atlantic Ocean. *Global Biogeochemical Cycles*, *29*(7), 1060–1074. https://doi.org/10.1002/2014GB005026

Rudels, B. (2019). Arctic Ocean circulation. In *Encyclopedia of ocean sciences* (3rd edn, pp. 262–277). Elsevier Inc. https://doi.org/10.1016/B978-0-12-409548-9.11209-6

Rudels, B., Björk, G., Nilsson, J., Winsor, P., Lake, I., & Nohr, C. (2005). The interaction between waters from the Arctic Ocean and the Nordic Seas North of Fram Strait and along the East Greenland current: Results from the Arctic Ocean-02 oden expedition. *Journal of Marine Systems*, *55*(1–2), 1–30. https://doi.org/10.1016/j.jmarsys.2004.06.008

Rutgers van der Loeff, M., Cai, P., Stimac, I., Bauch, D., Hanfland, C., Roeske, T., & Moran, S. B. (2012). Shelf-basin exchange times of Arctic surface waters estimated from 228Th/228Ra disequilibrium. *Journal of Geophysical Research*, *117*(C3), C03024. https://doi.org/10.1029/2011JC007478

Rutgers van der Loeff, M., Kipp, L., Charette, M. A., Moore, W. S., Black, E., Stimac, I., et al. (2018). Radium isotopes Across the Arctic Ocean Show time Scales of water mass ventilation and increasing shelf inputs. *Journal of Geophysical Research: Oceans*, *123*(7), 4853–4873. https://doi.org/10.1029/2018JC013888

Rutgers van der Loeff, M. M., Key, R. M., Scholten, J., Bauch, D., & Michel, A. (1995). 228Ra as a tracer for shelf water in the Arctic Ocean. *Deep-Sea Research II*, *42*(6), 1533–1553. https://doi.org/10.1016/0967-0645(95)00053-4

Rutgers van der Loeff, M. M., Stimac, I., Valk, O., Geibert, W., & Vieira, L. H. (2021a). *Radium isotopes and 228Th in surface water samples collected on POLARSTERN expedition PS100* [Dataset]. https://doi.org/10.1594/PANGAEA.936029

Rutgers van der Loeff, M. M., Stimac, I., Valk, O., Geibert, W., & Vieira, L. H. (2021b). *Radium isotopes and 228Th in water column samples collected on POLARSTERN expedition PS100* [Dataset]. https://doi.org/10.1594/PANGAEA.936027

Ryan-Keogh, T. J., Macey, A. I., Nielsdóttir, M. C., Lucas, M. I., Steigenberger, S. S., Stinchcombe, M. C., et al. (2013). Spatial and temporal development of phytoplankton iron stress in relation to bloom dynamics in the high-latitude North Atlantic Ocean. *Limnology & Oceanography*, *58*(2), 533–545. https://doi.org/10.4319/lo.2013.58.2.0533

Saito, M. A., & Moffett, J. W. (2001). Complexation of cobalt by natural organic ligands in the Sargasso Sea as determined by a new high-sensitivity electrochemical cobalt speciation method suitable for open ocean work. *Marine Chemistry*, *75*(1–2), 49–68. https://doi.org/10.1016/S0304-4203(01)00025-1

Sanders, J. G., Sanders, J. G., & Ryther, J. H. (1981). Dominance of a stressed marine phytoplankton Assemblage by a copper-tolerant pennate diatom. *Botanica Marina*, *24*(1), 39–42. https://doi.org/10.1515/botm.1981.24.1.39

Santschi, P. H., Murray, J. W., Baskaran, M., Benitez-Nelson, C. R., Guo, L. D., Hung, C. C., et al. (2006). Thorium speciation in seawater. *Marine Chemistry*, *100*(3–4), 250–268. https://doi.org/10.1016/j.marchem.2005.10.024

Schaffer, J., Kanzow, T., von Appen, W. J., von Albedyll, L., Arndt, J. E., & Roberts, D. H. (2020). Bathymetry constrains ocean heat supply to Greenland's largest glacier tongue. *Nature Geoscience*, *13*(3), 227–231. https://doi.org/10.1038/s41561-019-0529-x

Schaffer, J., Timmermann, R., Erik Arndt, J., Savstrup Kristensen, S., Mayer, C., Morlighem, M., & Steinhage, D. (2016). A global, high-resolution data set of ice sheet topography, cavity geometry, and ocean bathymetry. *Earth System Science Data*, *8*(2), 543–557. https://doi.org/10.5194/essd-8-543-2016

Schauer, U. (2016). The expedition PS94 of the research vessel POLARSTERN to the central Arctic Ocean in 2015. *Berichte zur Polar und Meeresforschung (Reports on Polar and Marine Research)* (Vol. 703). https://doi.org/10.2312/BzPM_0703_2016

Schlitzer, R. (2021). *Ocean Data View*. Retrieved from https://odv.awi.de

Schlitzer, R., Anderson, R. F., Dodas, E. M., Lohan, M., Geibert, W., Tagliabue, A., et al. (2018). The GEOTRACES intermediate data product 2017. *Chemical Geology*, *493*, 210–223. https://doi.org/10.1016/j.chemgeo.2018.05.040

Schmidt, G. A., Bigg, G. R., & Rohling, E. J. (1999). Global seawater oxygen-18 database [Dataset]. Retrieved from https://data.giss.nasa.gov/o18data/

Schulze, L. M., & Pickart, R. S. (2012). Seasonal variation of upwelling in the Alaskan Beaufort Sea: Impact of sea ice cover. *Journal of Geophysical Research*, *117*(C6), C06022. https://doi.org/10.1029/2012JC007985

Slagter, H. A., Reader, H. E., Rijkenberg, M. J. A., Rutgers van der Loeff, M., de Baar, H. J. W., & Gerringa, L. J. A. (2017). Organic Fe speciation in the Eurasian Basins of the Arctic Ocean and its relation to terrestrial DOM. *Marine Chemistry*, *197*, 11–25. https://doi.org/10.1016/j.marchem.2017.10.005

Smedsrud, L. H., Halvorsen, M. H., Stroeve, J. C., Zhang, R., & Kloster, K. (2017). Fram Strait Sea ice export variability and September Arctic Sea ice extent over the last 80 years. *The Cryosphere*, *11*(1), 65–79. https://doi.org/10.5194/tc-11-65-2017

Sunda, W. G., & Huntsman, S. A. (1988). Effect of sunlight on redox cycles of manganese in the southwestern Sargasso Sea. *Deep Sea Research Part A, Oceanographic Research Papers*, *35*(8), 1297–1317. https://doi.org/10.1016/0198-0149(88)90084-2

Sunda, W. G., & Huntsman, S. A. (1994). Photoreduction of manganese oxides in seawater. *Marine Chemistry*, *46*(1–2), 133–152. https://doi.org/10.1016/0304-4203(94)90051-5

Taylor, R. L., Semeniuk, D. M., Payne, C. D., Zhou, J., Tremblay, J.-É., Cullen, J. T., & Maldonado, M. T. (2013). Colimitation by light, nitrate, and iron in the Beaufort Sea in late Summer. *Journal of Geophysical Research: Oceans*, *118*(7), 3260–3277. https://doi.org/10.1002/jgrc.20244

Thornalley, D. J. R., Oppo, D. W., Ortega, P., Robson, J. I., Brierley, C. M., Davis, R., et al. (2018). Anomalously weak Labrador Sea convection and Atlantic overturning during the past 150 years. *Nature*, *556*(7700), 227–230. https://doi.org/10.1038/s41586-018-0007-4

Tonnard, M., Planquette, H., Bowie, A. R., van der Merwe, P., Gallinari, M., Desprez de Gésincourt, F., et al. (2020). Dissolved iron in the North Atlantic Ocean and Labrador Sea along the GEOVIDE section (GEOTRACES section GA01). *Biogeosciences*, *17*, 917–943. https://doi.org/10.5194/bg-2018-147

Torres-Valdés, S., Tsubouchi, T., Bacon, S., Naveira-Garabato, A. C., Sanders, R., McLaughlin, F. A., et al. (2013). Export of nutrients from the Arctic Ocean. *Journal of Geophysical Research: Oceans*, *118*(4), 1625–1644. https://doi.org/10.1002/jgrc.20063

Tovar-Sánchez, A., Duarte, C. M., Alonso, J. C., Lacorte, S., Tauler, R., & Galban-Malagón, C. (2010). Impacts of metals and nutrients released from melting multiyear Arctic Sea ice. *Journal of Geophysical Research*, *115*(C7), C07003. https://doi.org/10.1029/2009JC005685

Trimble, S. M., Baskaran, M., & Porcelli, D. (2004). Scavenging of thorium isotopes in the Canada Basin of the Arctic Ocean. *Earth and Planetary Science Letters*, *222*(3–4), 915–932. https://doi.org/10.1016/j.epsl.2004.03.027

Tsubouchi, T., Bacon, S., Aksenov, Y., Garabato, A. C. N., Beszczynska-Möller, A., Hansen, E., et al. (2018). The Arctic Ocean seasonal cycles of heat and freshwater fluxes: Observation-based inverse estimates. *Journal of Physical Oceanography*, *48*(9), 2029–2055. https://doi.org/10.1175/JPO-D-17-0239.1

Tsubouchi, T., Våge, K., Hansen, B., Larsen, K. M. H., Østerhus, S., Johnson, C., et al. (2021). Increased ocean heat transport into the Nordic Seas and Arctic Ocean over the period 1993–2016. *Nature Climate Change*, *11*(1), 21–26. https://doi.org/10.1038/s41558-020-00941-3

Twining, B. S., Nodder, S. D., King, A. L., Hutchins, D. A., LeCleir, G. R., DeBruyn, J. M., et al. (2014). Differential remineralization of major and trace elements in sinking diatoms. *Limnology & Oceanography*, *59*(3), 689–704. https://doi.org/10.4319/lo.2014.59.3.0689

Valk, O., Rutgers van der Loeff, M. M., Geibert, W., Gdaniec, S., Rijkenberg, M. J. A., Moran, S. B., et al. (2018). Importance of hydrothermal vents in scavenging removal of 230Th in the Nansen Basin. *Geophysical Research Letters*, *45*(19), 10539–10548. https://doi.org/10.1029/2018GL079829

Vance, D., Archer, C., Bermin, J., Perkins, J., Statham, P. J., Lohan, M. C., et al. (2008). The copper isotope geochemistry of rivers and the oceans. *Earth and Planetary Science Letters*, *274*(1–2), 204–213. https://doi.org/10.1016/j.epsl.2008.07.026

Van Den Berg, C. M. G., & Nimmo, M. (1987). Determination of interactions of nickel with dissolved organic material in seawater using cathodic stripping voltammetry. *The Science of the Total Environment*, *60*(C), 185–195. https://doi.org/10.1016/0048-9697(87)90415-3

van Ooijen, J., Rijkenberg, M. J. A., Gerringa, L. J. A., Rabe, B., & Rutgers Van Der Loeff, M. M. (2016). Inorganic nutrients measured on water bottle samples during POLARSTERN cruise PS94 [Dataset]. (ARK-XXIX/3). https://doi.org/10.1594/PANGAEA.868396

Vernet, M., Ellingsen, I. H., Seuthe, L., Slagstad, D., Cape, M. R., & Matrai, P. A. (2019). Influence of phytoplankton advection on the productivity along the Atlantic water inflow to the Arctic Ocean. *Frontiers in Marine Science*, *6*, 583. https://doi.org/10.3389/fmars.2019.00583

Vieira, L. H., Achterberg, E. P., Scholten, J., Beck, A. J., Liebetrau, V., Mills, M. M., & Arrigo, K. R. (2019). Benthic fluxes of trace metals in the Chukchi Sea and their transport into the Arctic Ocean. *Marine Chemistry*, *208*, 43–55. https://doi.org/10.1016/j.marchem.2018.11.001

von Appen, W. J., Schauer, U., Somavilla, R., Bauerfeind, E., & Beszczynska-Möller, A. (2015). Exchange of warming deep waters across Fram Strait. *Deep-Sea Research Part I Oceanographic Research Papers*, *103*, 86–100. https://doi.org/10.1016/j.dsr.2015.06.003

Wang, Q., Wekerle, C., Wang, X., Danilov, S., Koldunov, N., Sein, D., et al. (2020). Intensification of the Atlantic water supply to the Arctic Ocean through Fram Strait induced by Arctic Sea Ice decline. *Geophysical Research Letters*, *47*(3), e2019GL086682. https://doi.org/10.1029/2019GL086682

Wang, S., Bailey, D., Lindsay, K., Moore, J. K., & Holland, M. (2014). Impact of sea ice on the marine iron cycle and phytoplankton productivity. *Biogeosciences*, *11*(17), 4713–4731. https://doi.org/10.5194/bg-11-4713-2014

Weber, T., John, S., Tagliabue, A., & DeVries, T. (2018). Biological uptake and reversible scavenging of zinc in the global ocean. *Science*, *361*(6397), 72–76. https://doi.org/10.1126/science.aap8532

Wefing, A. M., Christl, M., Vockenhuber, C., Rutgers van der Loeff, M., & Casacuberta, N. (2019). Tracing Atlantic waters Using 129I and 236U in the Fram Strait in 2016. *Journal of Geophysical Research: Oceans*, *124*(2), 882–896. https://doi.org/10.1029/2018JC014399

Wehrmann, L. M., Formolo, M. J., Owens, J. D., Raiswell, R., Ferdelman, T. G., Riedinger, N., & Lyons, T. W. (2014). Iron and manganese speciation and cycling in glacially influenced high-latitude Fjord sediments (West Spitsbergen, Svalbard): Evidence for a benthic recycling-transport mechanism. *Geochimica et Cosmochimica Acta*, *141*, 628–655. https://doi.org/10.1016/j.gca.2014.06.007

Williams, W. J., & Carmack, E. C. (2015). The "interior" shelves of the Arctic Ocean: Physical oceanographic setting, climatology and effects of sea-ice retreat on cross-shelf exchange. *Progress in Oceanography*, *139*, 24–41. https://doi.org/10.1016/j.pocean.2015.07.008

Wilson, C., Aksenov, Y., Rynders, S., Kelly, S. J., Krumpen, T., & Coward, A. C. (2021). Significant variability of structure and predictability of Arctic Ocean surface pathways affects basin-wide connectivity. *Communications Earth & Environment*, *2*(1), 164. https://doi.org/10.1038/s43247-021-00237-0

Wilson, N., Straneo, F., & Heimbach, P. (2017). Satellite-derived submarine melt rates and mass balance (2011–2015) for Greenland's largest remaining ice tongues. *The Cryosphere*, *11*(6), 2773–2782. https://doi.org/10.5194/tc-11-2773-2017

Wu, M., McCain, J. S. P., Rowland, E., Middag, R., Sandgren, M., Allen, A. E., & Bertrand, E. M. (2019). Manganese and iron deficiency in Southern Ocean Phaeocystis Antarctica populations revealed through taxon-specific protein indicators. *Nature Communications*, *10*(1), 3582. https://doi.org/10.1038/s41467-019-11426-z

Wuttig, K., Townsend, A. T., van der Merwe, P., Gault-Ringold, M., Holmes, T., Schallenberg, C., et al. (2019). Critical evaluation of a seaFAST system for the analysis of trace metals in marine samples. *Talanta*, *197*, 653–668. https://doi.org/10.1016/j.talanta.2019.01.047

Zhang, R., John, S. G., Zhang, J., Ren, J., Wu, Y., Zhu, Z., et al. (2015). Transport and reaction of iron and iron stable isotopes in glacial meltwaters on Svalbard near Kongsfjorden: From rivers to estuary to ocean. *Earth and Planetary Science Letters*, *424*, 201–211. https://doi.org/10.1016/j.epsl.2015.05.031